ERG1a K^+ Channel Increases Intracellular Calcium Concentration through Modulation of Calsequestrin 1 in C_2C_{12} Myotubes

Gregory H. Hockerman[1,7], Evan Pratt[1,7], Shalini Guha[2], Emily LaVigne[1], Clayton Whitmore[2], Omar Khader[2], Natalie McClure[2], Sandra Zampieri[3,4], Jennifer Koran[5], W-H Wang[6], Amber L. Pond[2,8].

[1]Medicinal Chemistry and Molecular Pharmacology Dept., Purdue University School of Pharmacy, West Lafayette, IN 47906, USA; [2]Anatomy Dept., Southern Illinois University School of Medicine, Carbondale, IL 62902, USA; [3]Department of Surgery, Oncology and Gastroenterology, University of Padova, Padova, Italy; [4]Department of Biomedical Sciences, University of Padova, Italy; [5]School of Education, SIU Carbondale, IL; [6]Genetic Editing Core Facility, Purdue University, West Lafayette, IN.

[7]These authors contributed equally to the manuscript.

[8]Corresponding Author: Anatomy Dept., Southern Illinois University, Life Sciences Building III, Room 2080, 1135 Lincoln Drive, Carbondale, IL 62902; apond@siumed.edu

Key Words: ether-a-gogo related K^+ channel, skeletal muscle, intracellular calcium, RYR1, store operated calcium entry, calsequestrin 1

ABSTRACT

The ERG1A K^+ channel modulates the protein degradation that contributes to skeletal muscle atrophy by increasing intracellular calcium concentration ($[Ca^{2+}]_i$) and enhancing calpain activity, but the mechanism by which the channel regulates the $[Ca^{2+}]_i$ is not known. Here, we have investigated the effect of human ERG1A (HERG) on $[Ca^{2+}]_i$ in C_2C_{12} myotubes, using fura-2 calcium assays, immunoblot, RT-qPCR, and electrophysiology. We hypothesized that HERG would modulate L-type calcium channel activity, specifically the Cav1.1 channel known to carry signal from the sarcoplasmic membrane of skeletal muscle to the sarcomeres of the myofibrils. However, we find that HERG has no effect on the amplitude of L-type channel current nor does it affect the mRNA levels nor protein abundance of the Cav1.1 channel. Instead we find that, although the rise in $[Ca^{2+}]_i$ (induced by depolarization) is greater in myotubes over-expressing HERG relative to controls, it is not sensitive to the L-type channel blocker nifedipine, which suggests that HERG modulates excitation coupled calcium entry (ECCE). Indeed, the HERG-enhanced increase in $[Ca^{2+}]_i$ induced by depolarization is blocked by 2-APB, an inhibitor of ECCE. Further we discovered that HERG also modulates store operated calcium entry and the activity of ryanodine receptors. Therefore, we decided to investigate the effect of HERG on calsequestrin 1, a calcium buffering/binding protein known to modulate ryanodine receptor 1 and store operated Ca^{2+} entry activities. Indeed, we find that calsequestrin 1 mRNA levels are decreased by 17% ($p<0.05$) and the total protein abundance is lowered 77% ($p<0.05$) in myotubes over-expressing HERG relative to controls. In summary, the data show that ERG1A overexpression modulates $[Ca^{2+}]_i$ in skeletal muscle cells by lowering the abundance of the calcium buffering/binding protein calsequestrin 1.

INTRODUCTION

The *ether-a-go-go related gene* (*erg1*) encodes a number of ERG1 K^+ channel alpha subunit alternative splice variants. Two ERG1 splice variants, which have been cloned from both human ERG1 (HERG1A and 1B; London et. al., 1997) and mouse *Erg1* (*Merg1a* and *1b*; Lees-Miller et. al., 1997) cDNA libraries, form a heteromultimeric channel in mammalian heart. This ERG1A/1B channel has been shown to produce $I_{Kr,}$ a current which is partially responsible for late phase repolarization of the cardiac action potential (Jones, et. al., 2004; Curran et al., 1995). We have shown that the ERG1A K^+ channel subunit contributes to skeletal muscle loss in atrophic situations through up-regulation of ubiquitin proteasome proteolysis (UPP); we do not detect ERG1B in skeletal muscle (Wang et. al., 2006). Specifically, our labs have reported that the ERG1A K^+ channel is up-regulated in skeletal muscle of mice undergoing atrophy as a result of hind limb unweighting (Wang et. al., 2006), tumor-induced cachexia (Wang et al., 2006; Zampieri et al., 2021), and denervation (Anderson et. al., 2021). Moreover, we have reported that: 1) pharmacological and genetic block of ERG1A function inhibit skeletal muscle atrophy induced by hind limb suspension (Wang et. al., 2006); 2) atrophy is induced in mouse muscle by ectopic expression of wild type *Erg1a* (Wang et. al., 2006); and 3) abundance of the UPP E3 ubiquitin ligase MuRF1 (but not ATROGIN1) and overall UPP activity are increased in mouse skeletal muscle by ectopic overexpression of *Erg1a* (Hockerman et al., 2014; Pond et al., 2013; Wang et al., 2006). Further, we have shown that the ERG1A K^+ channel protein is expressed at low abundance in C_2C_{12} myotubes and that augmentation of its expression in these cells, as in mouse skeletal muscle, will induce a decrease in cell size (i.e., myotube area) and an increase in the abundance of the E3 ubiquitin ligase MuRF1, but not the E3 ligase ATROGIN1 (Whitmore et al., 2020). Finally, human ERG1A (HERG) expression in C_2C_{12} myotubes induces an increase

in basal intracellular calcium ($[Ca^{2+}]_i$) and calpain activity at 48 hours after transduction (Whitmore et. al., 2020). Thus, upregulation of ERG1A drives skeletal muscle atrophy *in vivo*, and ectopic expression of HERG1a in C_2C_{12} myotubes induces an atrophic phenotype *in vitro*.

Given the potentially important role of Ca^{2+} in modulation of skeletal muscle atrophy, we sought to understand the mechanism whereby HERG expression elevates basal $[Ca^{2+}]_i$ in C_2C_{12} myotubes (Whitmore et. al., 2020). Intracellular Ca^{2+} is essential for excitation-contraction coupling (ECC) in skeletal muscle. Specifically, $Ca_v1.1$ L-type voltage-gated Ca^{2+} channels (also known as dihydropyridine receptors, DHPR) are activated by the depolarizing action potentials that spread longitudinally along the muscle sarcolemma and inwardly into the myofibers along the t-tubules, where they are juxtaposed to ryanodine receptors 1 (RYR1). Through a physical interaction, the RYR1 and Cav1.1 together allow release of Ca^{2+} from the sarcoplasmic reticulum (SR) into the cytosol through the RYR1 channel. This increase in $[Ca^{2+}]_i$ (μM range) triggers skeletal muscle contraction, which is reversed when Ca^{2+} is "pumped" back into the SR by Ca^{2+}-ATPase (SERCA) (reviewed in Cho et. al., 2017). Smaller increases in $[Ca^{2+}]_i$ (nM range) also occur and these modulate muscle cell events such as upregulation of muscle thermogenesis in non-contracting muscle in response to cold (Bal et. al., 2012) and increase of both fatigue resistance and mitochondrial biogenesis (Bruton et. al., 2010). Localized Ca^{2+} concentration fluctuations also serve as second messengers, modulating numerous signaling systems (Tu et. al., 2016). Thus, $[Ca^{2+}]_i$ is affected by mechanisms other than the physical interaction between Cav1.1 and RYR1 that occurs in response to sarcolemmal membrane depolarization (i.e., ECC). One mode of Ca^{2+} modulation which results in relatively small changes in $[Ca^{2+}]_i$ is termed excitation coupled Ca^{2+} entry (ECCE); this Ca^{2+} influx is activated in response to prolonged and repetitive depolarization through a Cav1.1 and RYR1-mediated

interaction. The ECCE is activated in response to repeated or prolonged depolarization (e.g., by treatment with mM KCl *in vitro*), but is insensitive to the L-type channel blocking reagent nifedipine (Yang et. al., 2007). It is inhibited by 2-APB, which also blocks store operated Ca^{2+} entry (SOCE) and IP_3 receptors at the concentrations we used (100 μM), but is not affected by store depletion (Cherednichenko et. al., 2004; Hurne et. al., 2005). ECCE requires both RYR1 and Cav1.1 proteins, although L-type channel pore permeation is not necessary (Cherednichenko et. al., 2004); thus, researchers predict that this extracellular entry mechanism requires another (as yet unidentified) sarcolemmal Ca^{2+} channel. To date, it has been shown that Orai1 (Lyfenko and Dirksen 2008) and TRPC3 (Lee et. al., 2006) are not candidates. Calcium is also brought into the cell from the extracellular milieu through SOCE. SOCE is inhibited by depolarization and is activated by depletion of intracellular Ca^{2+} stores (i.e., the SR) (Kurebayashi & Ogawa 2001). Specifically, SR depletion results in dimerization of two SR membrane STIM1 proteins which then translocate through the SR membrane to interact with and open the sarcolemmal membrane Orai1 Ca^{2+} channel through which the Ca^{2+} moves into the cell from the extracellular milieu (Roos et. al., 2005; Feske et. al., 2006; Vig et. al., 2006).

Here, we show that, relative to controls, HERG-overexpression in myotubes enhances ECCE and SOCE activities and activity of the SR localized RYR1 Ca^{2+} channel. Coincidently, the abundance of the Ca^{2+} buffering protein calsequestrin1 (CalSeq1) is significantly lower in HERG-expressing myotubes than in control cells. Because RYR1 and SOCE activities are inhibited by CalSeq1 at higher concentrations of $[Ca^{2+}]_i$ (Jeong et. al., 2021; Zhang et al., 2016; Wang et. al., 2015; Wei et. al., 2009), the down regulation of CaSeq1 by HERG expression could enhance $[Ca^{2+}]_i$ by increasing the open probability of the RYR1 channel and by stimulating the ECCE and SOCE pathways.

MATERIALS AND METHODS

Cell Culture. C_2C_{12} cells (ATCC; Manassas, VA) were cultured in DMEM (ThermoFisher Scientific; Waltham, MA) containing 25 mM glucose, 4 mM L-glutamine and 3.7 g/L sodium bicarbonate and supplemented with 10% fetal bovine serum (FBS; ThermoFisher Scientific) within a 37°C incubator containing 6.5% CO_2. Differentiation of myoblasts into myotubes was induced by switching to culture medium as described here except that the 10% FBS was replaced with 2% heat-inactivated horse serum. After replacement of medium, cells were allowed to differentiate for 7-8 days at which point myotubes were transduced and allowed to incubate another 48 hours (i.e., another 2 days to produce 9-10 days cultured cells).

Antibodies. For Calsequestrin 1 immunoblots, the Calsequestrin 1 D-10 (sc-137080; Santa Cruz, Dallas, TX) mouse monoclonal antibody was used at a 1:100 dilution in PBS (pH 7.4) with 5% normal goat serum, 0.1% Triton X-100, and 0.01% sodium azide. To detect Cav1.1 α1 protein, the DHPR α1 antibody (MA3-920; ThermoScientific) was used at a 1:500 dilution in the buffer described above. For GAPDH protein immunoblots, we probed the membranes with a monoclonal antibody (Clone 6C5, MilliporeSigma; St. Louis, MO) diluted 1:8000 in Tris Buffered Saline (pH 7.4) containing 0.1% Tween-20 (TTBS) and 0.2% non-fat dry milk. The alkaline phosphatase conjugated goat anti-mouse IgG antibody (BioRad; Hercules, CA) was used as secondary antibody (with all of the primary antibodies described here) at 1:10,000 in blotting buffer (0.2% non-fat dry milk or casein and 0.1% Tween-20 in Tris Buffered Saline, pH 7.4; Sigma; St. Louis, MO).

Virus. The human ERG1A construct (Lin et al., 2010), was cloned into a viral cassette provided by ViraQuest, Inc. (North Liberty, IA) and then cloned by this company into the VQad CMV

adenovirus (containing GFP expression apparati). The appropriate control virus was also purchased from this company and used for the control transfections. Both sets of viral particles were maintained at -80°C until use.

Viral Transfection of C_2C_{12} Myotubes. HERG and control viral particles were added to DMEM with 2% horse serum (Gibco/ThermoFisher; Waltham, MA) and mixed. This suspension was used to treat C_2C_{12} myotubes (cultured as described above) at 200 multiplicity of infection (MOI) as pre-determined by titration, except that the myotubes used for the calsequestrin and GAPDH immunoblots in Fig. 7 were treated with 400 MOI. The virus treated plates were gently agitated to properly disperse the viral particles and then returned to the incubator. Viral expression as monitored by GFP fluorescence was detected at 24 hours post transfection and appeared to plateau at 48 hours when procedures were performed.

Intracellular Calcium Concentration Determinations. A Fura-2 QBT Calcium Kit (Molecular Devices; San Jose, CA) was used to assess $[Ca^{2+}]_i$ according to manufacturer's instructions. Briefly, myotubes were loaded with Fura-2 QBT by incubation with 1:1 Gibco Opti-MEM (Life Technologies; Carlsbad, CA) and Fura-2 QBT dissolved in modified Krebs-Ringer Buffer with HEPES (mKRBH; 0.05% fatty acid free bovine serum albumin in 134 mM NaCl, 3.5 mM KCl, 1.2 mM K_2HPO_4, 0.5 mM $MgSO_4$, 1.5 mM $CaCl_2$, 5 mM $NaHCO_3$, 10 mM HEPES) for 1 hour at room temperature (RT) in the dark. The medium was then replaced with Fura-2 QBT solution (in mKRBH) containing either a treatment (as described below) or vehicle (as control) and incubated at RT in the dark for 30 minutes. A Synergy MX Microplate Reader (BioTek; Winooski, VT) was used in conjunction with Genesis 2.0 software to excite the samples at 340 nm and 380 nm and to measure emission at 508 nm. The 340/380 nm ratio was determined and normalized to background as an assay for $[Ca^{2+}]_i$.

Depolarization Assays. Myotubes were cultured and treated with either control virus or virus encoding HERG as described earlier. At 48 hours post viral transduction, these myotubes were loaded with Fura-2 QBT and then treated with either vehicle or drug for 30 minutes. The drug was either: nicardipine (10 uM, an L-type Ca^{2+} channel blocker), nifedipine (10 μM, an L-type Ca^{2+} channel blocker), thapsigargin (TG, 1 uM, an inhibitor of SERCA1), 2-aminoethoxydiphenyl borate (2-APB; 100 μM to block SOCE, ECCE, and IP3R; Sigma), or astemizole (1 nM, a HERG channel blocker). The fluorescence assay for $[Ca^{2+}]_i$ (as described above) was started for one minute (to determine background) and then the cells were depolarized with 100 mM KCl and assayed for an additional 2.5 minutes.

Ryanodine Receptor Assays. Myotubes were cultured and treated with either control virus or virus encoding HERG as described earlier. At 48 hours post viral transduction, the myotubes were loaded with Fura-2 QBT and then treated for 30 minutes with ryanodine (90 μM, as determined by a dose-response curve to completely block caffeine induced Ca^{2+} release; data not shown) to block RYR1. The Fura-2 QBT $[Ca^{2+}]_i$ assay (as described above) was started for one minute and then the cells were treated with caffeine (5 mM) to activate RYR1 and assayed for an additional 2.5 minutes.

SOCE Assays. Myotubes were cultured and treated with either control virus or virus encoding HERG as described earlier. At 48 hours post viral transduction, the myotubes were treated with either vehicle or 2-APB (100 μM; to block SOCE activity) for 30 minutes. The cells were then assayed for $[Ca^{2+}]$i using Fura-2 QBT as described above. After 1 minute of assay, an aliquot of vehicle or TG (final 1 μM to "empty" the SR stores) was dispensed into the wells and $[Ca^{2+}]_i$ was assayed for an additional 20 minutes to ensure Ca^{2+} levels were consistently low. At 20

minutes, Ca^{2+} (final 2.5 mM $CaCl_2$) was added to activate SOCE and the cells were assayed for an additional 10 minutes.

RNA Isolation and RT-qPCR. Total RNA was extracted from control and HERG-expressing C_2C_{12} myotubes using Trizol reagent (Life Technologies; Carlsbad, CA) according to manufacturer's instructions followed by chloroform solubilization and ethanol precipitation. RT-qPCR (quantitative reverse transcriptase PCR) was then performed using a Luna® Universal One-Step RT-qPCR Kit (New England Biolabs; E3005) per manufacturer's instructions and primers for the CaSeq1 gene of interest (IDT; San Jose, CA) along with primers for ERG1A (Invitrogen; Waltham, MA) and the GAPDH "housekeeping gene" (IDT) (Table 1). A CFX BioRad OPUS 96 real time PCR system was used to detect SYBR green fluorescence as a measure of amplicon. Changes in gene expression were determined using the Livak method to normalize the gene of interest to the "housekeeping gene." No template controls (NTC) and no-reverse transcriptase (no-RT) controls were also assayed along with our samples of interest in each set of PCR reactions.

Cell Lysate Preparation and Protein Assay. C_2C_{12} cells were differentiated in 10 cm plates for 7-8 days and then transduced with either control or HERG-encoded virus and incubated an additional 48 hours (2 days). Membrane proteins were extracted from myotubes by gently washing tissue culture plates twice with room temperature PBS and then scraping cells from the plates treated with 250 μL of cold Tris-EDTA buffer (10 mM, 1 mM respectively, pH 7.3; Sigma) containing 2% Triton-X100 (Sigma) and protease inhibitors: 0.5 mM pefabloc, 1 mM benzamidine, 1 mM iodoacetamide, 1 mM 1,10-phenanthroline, and a commercial protease cocktail tablet (Pierce A32955 [ThermoFisher] used per manufacturer instructions). Cell suspensions were triturated with a 23-gauge needle and 1 mL syringe and then again with a 27-

gauge needle and 1 mL syringe. The samples were then allowed to sit on ice in a refrigerator for 20 minutes to enhance membrane solubilization. The cell lysates were then triturated with an Eppendorf pipette (200 uL tip) and centrifuged at 12,000xg for 10 minutes to remove solid material. Sample supernatants were collected and stored at -80°C.

Protein Determination. To determine sample protein concentration, a standard curve was developed using BSA (Sigma) and then a DC Protein Assay kit (BioRad; Carlsbad, CA) was used to develop color in the standards and samples from which protein content was determined by linear regression using Excel (Microsoft 365; Redmond, WA).

Immunoblot. For immunoblots, aliquots of equal protein content (40 ug) were boiled for 5 minutes with sample dilution buffer (5X SDB; 0.3 M Tris [pH 6.9], 50% glycerol, 5% SDS, 0.5 M dithiothreitol, and 0.2% bromophenol blue). Samples were then electrophoresed through a 4-20% polyacrylamide (SDS-PAGE) gradient gel, transferred to PVDF membrane (BioRad; Hercules, CA), and immunoblotted using antibodies specific for either: calsequestrin 1 or Cav1.1 (also called DHPR). Secondary antibodies conjugated with alkaline phosphatase were used with an ImmunStar™-Alkaline Phosphatase (AP) Western Chemiluminescent Kit (Bio-Rad) for signal development. To ensure that lanes were loaded equally, after development for CaSeq1 or Cav1.1 signal, PVDF membranes were incubated (30 minutes at room temperature) in stripping buffer (62.5mM Tris Cl [pH=6.9], 2% SDS, 0.695% BME in water), rinsed with 0.1% Tween 20 in 20 mM Tris (TTBS, pH 7.4) and re-probed with GAPDH antibody (see next section for imaging details). To further confirm protein loading equity, Coomassie Blue stain solution (0.1% Coomassie Blue R-250 in 45% methanol and 10% acetic acid in water) was used to stain the membranes overnight, after which these were destained with 50% methanol and 10% acetic acid in water.

Immunoblot Imaging. ImageJ (NIH; NC) was used to determine the optical densities of the protein bands: a single region of interest (ROI) which encompassed each protein band was outlined and this ROI was used to demarcate each protein band and a background area above each band. The average uncalibrated optical density (OD) was determined for each ROI and the background OD was subtracted from the OD of each target protein band (e.g., Cav1.1 and CaSeq1). The same was done for the internal reference GAPDH protein. Then to correct for any differences in sample loading, for each sample a ratio was calculated by dividing the background-corrected OD for each target protein by the background-corrected OD for GAPDH for each sample.

Electrophyisology: Barium Current Densities. C_2C_{12} myoblasts were seeded in 35 mm cell culture dishes, differentiated to myotubes, and transduced with either control eGFP encoded virus or HERG encoded virus as described. Micropipettes were pulled from borosilicate capillaries to an inside diameter of 3-5 microns using a Sutter P-87 pipette puller, and polished with a Narishige MF 830 microforge. The pipette solution contained (mM): 180 NMDG, 40 HEPES, 4 $MgCl_2$, 12 phosphocreatine, 5 BAPTA, 2 Na_2ATP, 0.5 Na_3GTP, 0.1 leupeptin, and pH was adjusted to 7.3. The extracellular solution contained (mM): 140 NaCl, 20 $CsCl_2$, 10 $BaCl_2$, 10 HEPES, 10 glucose, 10 sucrose, 1 $MgCl_2$, and pH was adjusted to 7.4. Voltage dependent barium currents were measured under voltage clamp using an Axopatch 200B amplifier (Axon Instruments). Data were sampled at 10 kHz and filtered at 1 kHz. Cells were held at -80 mV and stepped to test voltages ranging from -60 mV to +50 mV in 10 mV increments. Current densities (pA/pf) were calculated by dividing the largest current amplitude for each cell, regardless of test voltage, by the whole cell capacitance.

Statistics. Area under the curve (AUC) data were determined and all statistical analyses were performed using GraphPad Prism 9 (Dotmatics; Boston, MA). A Student's T-test was used to analyze the optical density data from the immunoblots, the Ca^{2+} current densities, and the HERG and calsequestrin 1 gene expression data. A one-way ANOVA was used to analyze the AUC data from the RyR1 and SOCE activity studies as well as the fold changes in Cav1.1 gene expression data. When significant differences were found, means were separated by Tukey's test. For the samples depolarized with KCl, the AUCs per time unit were determined and analyzed with a 2 x 2 ANOVA design for repeated measures and the interaction between HERG and treatment was examined for statistical significance. The drug sensitive currents were determined by calculating, for each time point, the difference between the means of the normalized 340:380 ratios of the drug treated and non-drug treated cells within each the HERG-expressing and the transduced control samples. The mean difference and the standard error of the mean difference (SEMD) were then calculated and used to estimate p values with a comparison of means calculator (MedCalc Software Ltd.; Belgium; https://www.medcalc.org/calc/comparison_of_means.php).

RESULTS

The HERG channel affects $[Ca^{2+}]_i$ by modulation of Excitation Coupled Calcium Entry.

Depolarization with KCl. HERG-expressing myotubes (Whitmore et. al., 2020 validates viral expression model; Fig. SD1) show a significantly higher intracellular Ca^{2+} concentration than control cells for ~1.5 minutes after depolarization with 100 mM KCl (Fig. 1A). *Nifedipine Block.* Nifedipine has a strong blocking effect on the increase in $[Ca^{2+}]_i$ that normally occurs in response to depolarization in the control cells, inhibiting ~67.5% of the rise in $[Ca^{2+}]_i$ at 20s and then lowering it substantially (over 90-103% blocked) from 40s to 120s (Fig. 1B). This demonstrates that a large portion of the increase in $[Ca^{2+}]_i$ that occurs in control C_2C_{12} myotubes in response to depolarization is a result of L-type channel activation. Nifedipine also has a strong effect on the rise in $[Ca^{2+}]_i$ that occurs in response to depolarization in the HERG-expressing myotubes. It blocks approximately 60, 73, and 77% of the Ca^{2+} increase that occurs initially (at 20, 30, and 40s, respectively; $p<0.05$) and then ranges from 70-42% from 50-120s (Fig. 1C). Although the nifedipine block does not appear as strong over time in the HERG-expressing cells, indeed, when the specific nifedipine-sensitive Ca^{2+} transients are determined and compared (Fig. 1D), there is no statistical difference in the initial nifedipine-sensitive response of the HERG-treated and control myotubes and virtually no difference beyond the initial ~10 seconds post depolarization. We obtained similar results with the L-type channel blocker nicardipine (data not shown). Thus, although HERG is inducing a greater increase in $[Ca^{2+}]_i$ in response to depolarization, this effect does not appear to be the result of increased Cav1.1 activity at 48 hours after transduction. We explored potential L-type channel involvement further. *L-Type Current Density.* Myotubes were transduced with either a HERG-encoded or an appropriate control virus and after 48 hours were evaluated for L-type current using whole-cell voltage

clamp of myotubes (see Methods). The data demonstrate that HERG had no effect on peak L-type channel Ba^{2+} current density (pA/pF) (Fig. 2A). *Skeletal Muscle L-Type Channel Gene Expression.* Control and HERG-expressing myotubes were assayed for expression of genes encoding $Ca_v1.1$, embryonic $Ca_v1.1$ (Cav1.1e), $Ca_v1.2$, and $Ca_v1.3$ using RT-qPCR. No significant differences were found in expression of any of these genes for up to 60 hours after transduction (Fig. 2 B,C; $Ca_v1.2$ and 1.3 data not shown). *Skeletal Muscle L-Type Channel α Subunit Protein Abundance.* Lysates from control and HERG-expressing myotubes were immunoblotted (Fig. 2 D) using an antibody specific for the skeletal muscle Cav1.1 channel α subunit and protein signal was detected by chemiluminescence. The ODs of the Cav1.1 protein band reveal that HERG had no effect on Cav1.1 protein abundance (Fig. 2 E). We find no effect of HERG on L-type current amplitude or Cav1.1 channel α subunit gene expression or protein abundance although HERG does increase myotube $[Ca^{2+}]_i$ (over controls) in response to depolarization. Indeed, the fact that the HERG-modulated response is activated by depolarization and is nifedipine insensitive implicates ECCE, a Ca^{2+} release pathway that is insensitive to store depletion. *2-APB Block with Depolarization.* To further test if HERG is modulating ECCE, control and HERG-expressing myotubes were treated with vehicle or 2-APB, which will block ECCE (and SOCE) (Olivera & Pizarro 2010), and then depolarized to activate ECCE (and inhibit SOCE) (Stiber et. al., 2008 in Dirksen 2009; Kurebayashi & Ogawa 2001). Time resolved assays of $[Ca^{2+}]_i$ using Fura-2 revealed that 2-APB inhibits the initial (up to 20 seconds) increase in $[Ca^{2+}]_i$ that occurs in response to depolarization in both control and HERG-overexpressing myotubes: HERG-overexpressing cells, 78.8% inhibition, $p<0.01$; control cells, 68.9% inhibition, $p<0.05$ (Fig. 3A,B). Indeed, the 2-APB sensitive response during initial treatment (10 s) was significantly greater (49.4%; $p<0.05$) in the HERG-expressing cells relative

to controls (Fig. 3C). Thus, these data suggest that HERG overexpression in C_2C_{12} myotubes modulates ECCE.

The HERG channel affects $[Ca^{2+}]_i$ by modulation of Store Operated Calcium Entry. The data strongly support that a source of the HERG-modulated increase in $[Ca^{2+}]_i$ in skeletal muscle cells is the ECCE; however, this does not rule out the possibility that HERG also modulates other Ca^{2+} entry pathways such as SOCE. Here, we assay SOCE (see methods) and quench ECCE by not depolarizing the cells. Briefly, we treated control and HERG-expressing cells with TG to deplete intracellular stores and thus activate SOCE. We then treated cells within each group with either 2-APB to block SOCE (and ECCE) or vehicle. Finally, we added extracellular Ca^{2+} (2.5 mM $CaCl_2$) to stimulate SOCE and monitored $[Ca^{2+}]_i$ with Fura-2. The AUC data show that $[Ca^{2+}]_i$ in HERG-expressing cells was significantly increased (68.2%; p=0.035) over controls (Fig. 4) in response to 2.5 mM extracellular $CaCl_2$. The 2-APB treatment did not inhibit the rise in $[Ca^{2+}]_i$ upon addition of 2.5 mM $CaCl_2$ in control myotubes. In contrast, 2-APB blocked the $[Ca^{2+}]_i$ increase that occurred in response to $CaCl_2$ in the HERG-expressing cells by a statistically significant 78.2% (p=0.0003). These data demonstrate that overexpression of HERG in C_2C_{12} myotubes results in a greater SOCE response to thapsigargin, either directly, or by HERG-enhanced depletion of SR stores.

The HERG channel modulates Ryanodine Receptor 1. *Thapsigargin Block with Depolarization.* To test if HERG could also be enhancing release of Ca^{2+} from intracellular stores, control and HERG-expressing myotubes were treated with either vehicle or TG, which will deplete intracellular stores and activate SOCE, but have no effect on ECCE (Cherednichenko et. al., 2004; Lyfenko & Dirksen 2008 in Dirksen 2009). The cells were then depolarized: 1) to release RYR1 from occlusion by $Ca_v1.1$ (i.e., DHPR) and enable Ca^{2+} release

from the SR to the cytosol through the RYR1 channel (Pitake and Ochs 2015); and 2) to inhibit SOCE (Stiber et. al., 2008 in Dirksen 2009; Kurebayashi & Ogawa 2001). Indeed, depolarization activates the ECCE and pre-treatment with TG will empty SR stores; thus, any inhibition noted in the TG treated groups relative to vehicle treated groups will be predominantly a consequence of lowered SR stores. Time resolved $[Ca^{2+}]_i$ assays using Fura-2 assays revealed thapsigargin did not significantly reduce the rise in $[Ca^{2+}]_i$ upon KCl depolarization in control cells (Fig. 5A). However, the depolarization-induced rise in $[Ca^{2+}]_i$ was significantly inhibited by thapsigargin in HERG-expressing myotubes relative to vehicle treated HERG-expressing myotubes for up to 40 seconds (20s, 49.4% decrease, $p<0.05$; 30s, 72.7%, $p<0.05$; 40s, 77.1%, $p<0.05$; Fig. 5B) after depolarization. Indeed, the TG-sensitive portion of the response to depolarization was greater in HERG-expressing cells, with the difference in the TG-sensitive response being statistically significant in earlier time points (~8-14s; Fig. 5C). These data strongly suggest that a source of increased $[Ca^{2+}]_i$ in the HERG-expressing myotubes is at least, in part, release of Ca^{2+} from SR stores. *Ryanodine Receptor Activation with Caffeine.* Membrane depolarization will uncouple RYR1 from occlusion by the DHPR and allow Ca^{2+} release from the SR to the cytosol through the RYR1 channel (Pitake and Ochs 2015); therefore, we determined if HERG affects RYR1 activity specifically. Thus, RYR1 activity was assayed in control and HERG-expressing myotubes using caffeine to activate the RYR1 and the area under the curve (AUC) of the rise in $[Ca^{2+}]_i$ was determined for each treatment group. Caffeine induced a statistically significant increase in $[Ca^{2+}]_i$ in both the control (2.7-fold increase; $p=0.0001$) and HERG-expressing (3.2-fold increase; $p<0.0001$) myotubes (Fig. 6). As expected, ryanodine (90 μM) blocked the increase in $[Ca^{2+}]_i$ stimulated by caffeine. However, the effect of ryanodine on the control cells was not significant, decreasing $[Ca^{2+}]_i$ by 24.9% ($p=0.34$) while ryanodine caused a statistically

significant 46.4% (p=0.0007) decrease in the $[Ca^{2+}]_i$ of HERG-expressing cells. The data demonstrate that HERG overexpression enhances caffeine-induced release of Ca^{2+} from the SR via RyR1 in C2C12 myotubes.

The HERG channel lowers abundance of Calsequestrin1 mRNA and protein. Calsequestrin 1 (CaSeq1) functions as both a Ca^{2+} buffer and a Ca^{2+} sensor in the SR and inhibits ryanodine receptor activity at cytosolic Ca^{2+} concentrations around 1 mM in skeletal muscle. It also inhibits the dimerization of the STIM1 protein necessary to activate the Orai1 channel for SOCE activity (Zhang et. al., 2016; Jeong et. al., 2021). Because the calsequestrin1 protein modulates RYR1 and STIM1, it has the potential to affect numerous pathways by which Ca^{2+} enters the cytosol, including via ECC, ECCE, and SOCE. Therefore, we explored the effect of HERG-expression on CaSeq1 levels in C_2C_{12} myotubes. Total RNA was extracted from both control and HERG-expressing myotubes transduced at 200 MOI (n=8, 4 control plates and 4 HERG plates) and HERG and CaSeq1 mRNA levels, relative to GAPDH, were compared using RT-qPCR. Myotubes transduced with adenovirus encoding HERG exhibited a 2.6-fold increase ($p<0.02$) in HERG mRNA and a 0.83-fold decrease ($p<0.05$) in CaSeq1 mRNA at 48 hours after transduction (Fig. 7A). Further, both control and HERG-expressing myotubes were transduced at 200 MOI (n=8, 4 control and 4 HERG) and lysates were immunoblotted using antibodies specific for either CaSeq1 or GAPDH (Suppl. Fig. 2). We measured the optical densities (OD) of the protein bands and noted a reduction in CaSeq1 protein (23.5%) that approached, but did not reach significance (p=0.081). To increase HERG expression levels, we transduced both control and HERG-expressing myotubes at 400 MOI (n=8, 4 control and 4 HERG) and immunoblotted the lysates (Fig. 7 B-E) with antibodies specific for CaSeq1 and then (after stripping) with GAPDH. We detected a full length CaSeq1 ~65 kD protein along with ~50 kD and ~40 kD

CaSeq1 proteins which appear to be CaSeq1 degradation products (Fig. 7B). The mean OD of each CaSeq1 protein band was decreased in the HERG-expressing myotubes relative to control cells: the ~65 kD protein decreased 89.7% ($p=0.012$); the ~50 kD protein decreased 66.3% ($p=0.077$); and the ~40 kD protein decreased 80.8% ($p=0.088$). When the OD values are combined per sample ("Total," Fig. 7E) and compared by a Student's t-test (HERG versus control), there is a 77% ($p=0.036$) decrease in CaSeq1 protein abundance in HERG transduced myotubes. These data show that HERG over-expression produces a decrease in CaSeq1 protein abundance.

DISCUSSION

Although ERG1A has been detected in the sarcolemma and t-tubules of heart muscle (Rasmussen et al., 2004; Jones et al., 2004), the presence of ERG1A in skeletal muscle was not reported until we detected it in the sarcolemma of atrophying skeletal muscle (Wang et al., 2006; Zampieri et. al., 2021). To determine if ERG1A expression plays a role in atrophy, we electro-transferred ERG1A cDNA into mouse *Gastrocnemius* muscle and discovered that the ERG1A-expressing fibers decreased in size. Thus, we hypothesized that ERG1A might contribute to atrophy (Wang et. al., 2006). Similarly, over-expression of ERG1A in cultured C_2C_{12} myotubes decreased myotube size compared to controls. Further, ERG1A did not produce a change in the fusion index, indicating that ERG1A likely does not affect differentiation (Whitmore et. al., 2020). Importantly, ERG1A did not increase either the number of centrally located nuclei or the abundance of laminin in these myotubes (Whitmore et. al., 2020), suggesting that ERG1A does not contribute to tissue degeneration. Thus, it is likely that ERG1A up-regulates protein degradation in myotubes, producing atrophy. Over-expression of ERG1A in mouse *Gastrocnemius* muscle enhances proteolysis through up-regulation of UPP activity by increasing both the mRNA level and protein abundance of the muscle specific UPP E3 ligase MuRF1 (Wang et. al., 2006; Pond et. al., 2013; Hockerman et. al., 2014). Finally, HERG-expression in C_2C_{12} myotubes produces an increase in MuRF1 protein abundance and, interestingly, in both basal $[Ca^{2+}]_i$ and calpain activity (Whitmore et. al., 2020). Because elevated $[Ca^{2+}]_i$ levels could potentially play a role in atrophy, we sought to determine by what mechanism(s) HERG regulates $[Ca^{2+}]_i$.

ERG1A is a sarcolemma membrane-bound voltage-gated K^+ channel, thus it is feasible that it might affect the L-type voltage-gated Ca^{2+} channel(s) also located in the sarcolemma. We

reasoned that the ERG1A channel would not likely hyperpolarize the skeletal myocyte membrane appreciably because it's role in cardiac tissue is to facilitate repolarization of the action potential and prevent early afterdepolarizations (Jones et al., 2014). We hypothesized, however, that the channel's presence in the skeletal muscle sarcolemma might in some way modulate the current amplitude or abundance of the Cav1.1 Ca^{2+} channels (DHPRs) located there. Indeed, when C_2C_{12} myotubes were depolarized with KCl (100 mM), they exhibited an increase in $[Ca^{2+}]_i$ in both control and HERG-expressing myotubes, which was significantly greater in the HERG-expressing cells for 80s post depolarization.

Typically, a large portion of the increase in $[Ca^{2+}]_i$ that occurs in response to depolarization in skeletal muscle is inhibited by L-type channel blockers such as nifedipine or nicardipine, as was the case in control C_2C_{12} myotubes when depolarized with KCl. However, the HERG-modulated increase in $[Ca^{2+}]_i$ that occurs in response to depolarization is not blocked by nifedipine or nicardipine, indicating it is not mediated by Ca^{2+} influx via L-type voltage-gated channels (e.g., skeletal muscle $Ca_v1.1$ channels). Our data suggest that HERG modulates ECCE activity, an extracellular Ca^{2+} entry pathway that is activated by prolonged and repetitive depolarization (e.g., KCl), but is not sensitive to block of the L-type channel pore with nifedipine. ECCE activity does require Cav1.1 channels; however, permeation of the L-type channel pore by Ca^{2+} is not necessary (reviewed in Dirksen 2009; Yang et.al., 2007; Cherednichnko et. al., 2004). The ECCE activity unit is believed to be composed of Cav1.1, RYR1, and an (as yet) unrevealed Ca^{2+} conducting channel (reviewed in Cho et. al., 2017 and in Dirksen 2009). Further evidence that ERG1A modulates ECCE activity is that the HERG-modulated, depolarization-induced increase in $[Ca^{2+}]_i$ is blocked by 2-APB, a compound known to block ECCE activity (Cherednichenko et. al., 2004). 2-APB also blocks Ca^{2+} entry from the extracellular milieu

through SOCE (Cherednichenko et. al., 2004); however, SOCE is inhibited by depolarization and activated by SR depletion (Kurebayashi & Ogawa 2001; Stiber et. al., 2008) and thus is not active in the depolarization-induced Ca^{2+} assay in which 2-APB treatment was applied. Further, no TG was present to deplete SR stores in this study. However, a portion of this HERG-modulated, depolarization-induced increase in $[Ca^{2+}]_i$ is sensitive to store depletion by TG. Indeed, ECCE activity is NOT affected by SR store depletion. Thus, the data suggest that HERG may also activate release of Ca^{2+} from intracellular stores (Cherednichenko et. al., 2004; Hurne et. al., 2005). Therefore, we tested if HERG has an effect on RYR1. It is reported that RYR1 is voltage-activated (Nelson et. al., 2013) and that membrane depolarization will release RYR1 from occlusion by the DHPR and allow Ca^{2+} release from the SR to the cytosol through the RYR1 channel (Pitake and Ochs 2015). Indeed, expression of HERG did enhance the increase in $[Ca^{2+}]_i$ that occurs with caffeine treatment in myotubes, and this effect was blocked by ryanodine, indicating HERG-modulation of RYR1. Further, our data show that HERG also modulates SOCE, which brings Ca^{2+} into the cytosol from the extracellular milieu in response to depletion of SR stores; however, our data do not indicate whether the modulation is a consequence of stores depletion subsequent to HERG-modulated RYR1 activation or of direct regulation of SOCE protein players.

Given our finding that ERG1A modulates both the ECCE and SOCE, as well as RYR activity (reviewed in Cho et. al., 2017 and Dirksen 2009), we conjectured that ERG1A could be affecting an entity that regulates all three Ca^{2+} entry pathways. We hypothesized that calsequestrin1, a Ca^{2+} sensing and buffering protein detected prominently within the SR milieu, would be a likely candidate. Indeed, our immunoblot data demonstrate that CaSeq1 protein abundance is significantly lower in HERG-expressing cells than in controls. Interestingly, CaSeq1 modulates

Ca^{2+} by interacting with RYR1: at ≥5mM Ca^{2+} concentration in the SR ($[Ca^{2+}]_{SR}$), CaSeq1 is polymerized and binds/stores high Ca^{2+} levels near the junctional SR membrane to allow quick release of Ca^{2+} during ECC; this action also buffers Ca^{2+} and regulates SR osmolarity (Perni et. al., 2013; reviewed in Woo et. al., 2020 and in Wang & Michalak 2020). At ~1mM $[Ca^{2+}]_{SR}$, although still polymerized and binding Ca^{2+} ions, CaSeq1 binds and inhibits RYR1 so that Ca^{2+} cannot pass through this channel into the cytosol (Beard et. al. 2005; Herzog et al., 2000). At $[Ca^{2+}]_{SR}$ ≤100 μM, CaSeq1 depolymerizes, thus lowering its Ca^{2+} binding capacity and releasing free Ca^{2+} with in the SR as it also dissociates from RYR1. The interaction between RYR1 and CaSeq1 requires other SR junctional proteins such as junctin and triadin in a quarternary complex. Removing CaSeq1 from the RYR1-junctin-triadin complex creates an increased probability and duration of RYR1 channel opening; adding the CaSeq1 back to this RYR1 complex yields decreased channel opening duration [(Beard et al., 2002; Beard et al., 2005]). Thus, CaSeq1 essentially blocks RYR1 activity at resting Ca^{2+} concentrations. Further, RYR1 is a component of ECCE and, although it is not believed to be the Ca^{2+}-passing entity in this extracellular Ca^{2+} entry pathway (reviewed in Dirksen 2009 and Cho et. al., 2017), ECCE activity is potentiated by ryanodine treatment: accentuated by low dose and blocked by high doses (Gach et. al., 2008; (Cherednichenko et. al., 2004, 2008). Thus, it is possible that the effect of ERG1A on ECCE is through CaSeq1 modulation of RYR1. It could also be through CaSeq1 modulation of Cav1.1. A complex of CaSeq1 and the transmembrane protein JP45 modulate Cav1.1 (Mosca et. al., 2013) and ablation of both JP45 and CaSeq1 proteins enhances ECCE activity in mouse skeletal muscle (Mosca et. al., 2016). However, as we demonstrate here, ERG1A modulation of Cav1.1 is not likely to occur. ERG1A could also be affecting $[Ca^{2+}]_i$ through CaSeq1 modulation of SOCE. CaSeq1 regulates SOCE by inhibiting STIM1

aggregation, thus decreasing the entry of Ca^{2+} through this extracellular pathway (Wang et al., 2015; Zhang et. al., 2016). CaSeq1 also inhibits STIM2 aggregation (Jeong et. al., 2021). Thus, down-regulation of CaSeq1 protein could play a role in skeletal muscle atrophy induced by ERG1A.

Work with CaSeq1 knockout mice work supports this conclusion. CalSeq1 knockout mice were viable, but skeletal muscle from these mice exhibited enhanced sensitivity to caffeine, an increased magnitude of Ca^{2+} release in response to depolarization, and an increase in resting $[Ca^{2+}]_i$, suggesting that CaSeq1 modulates RYR1 activity (Dainese et. al., 2009). Thus, these data support that a decrease in CaSeq1 would result in an increase in both resting $[Ca^{2+}]_i$ and Ca^{2+} release in response to depolarization. Further, CaSeq1 ablation results in formation of SR-stacks which contribute to formation of Ca^{2+} entry units (CEUs), which are intracellular junctions that modulate SOCE (Dainese et. al., 2009). These SR-t-tubule junctions within the I-band of CaSeq1 null mice muscle represent pre-assembled CEUs that provide a mechanism for constitutively active SOCE, hypothesized to be a calcium source compensating for the lower Ca^{2+} concentration within the SR (Boncompagni et al. 2012; 2018; Michelli 2019, 2020). Constitutively active SOCE could explain the increased basal intracellular Ca^{2+} detected in C_2C_{12} myotubes overexpressing HERG (Whitmore et. al., 2020). Interestingly, CaSeq1-ablated mice also presented with a reduction in body weight compared to wild type (WT) (Paolini et al., 2015; Paolini et al., 2007) and with skeletal muscle atrophy, which manifested as an average 37% decrease in EDL muscle fiber cross sectional area and a significantly reduced grip strength (Paolini et al., 2015). The atrophy is likely (at least partially) explained by the increase in expression of certain atrogenes (i.e., CathepsinL, Psmd1, Bnip3, and Atrogin) also reported by this group. It could also be (at least in part) a result of an increase in Ca^{2+} dependent calpain

activity induced by the increase in $[Ca^{2+}]_i$. These results are consistent with the finding that HERG overexpression in *Gastrocnemius* muscle and C_2C_{12} myotubes induces skeletal muscle atrophy (Wang et. al., 2006; Whitmore et. al., 2020).

One question left unanswered by this study is: How does ERG1A over-expression result in lowered CaSeq1 protein levels (Fig.8A)? ERG1A up-regulates UPP activity by increasing the abundance of the MuRF1 E3 ligase in mouse skeletal muscle and in C_2C_{12} myotubes (Whitmore et. al., 2020; Wang et. al., 2006). Therefore, we hypothesize that ERG1A may enhance the degradation of the CalSeq1 protein by increasing UPP activity, because there are ubiquitinylation sites on CalSeq1 (https://www.phosphosite.org/homeAction). It is also possible that ERG1A in some way interferes with CaSeq1 gene expression or post-transcriptional modulation. These areas remain to be explored. Perhaps the most fundamental question regarding the role of ERG1A in skeletal muscle atrophy is: "What induces increased levels of the ERG1A channel in skeletal muscle (Fig. 8B)?" ERG1A is up-regulated in skeletal muscle undergoing atrophy as a consequence of unloading, cancer cachexia and denervation (Zampieri et. al., 2021; Wang et al., 2006; Hockerman et al., 2013; Pond et al., 2014). It is likely, therefore, that some factor common to these conditions induces expression of ERG1A. Perhaps simply a decrease in stimulation of the muscle contributes in some way. This is another area that remains to be explored.

This study may have relevance to muscle pathologies other than atrophy because increases in $[Ca^{2+}]_i$ can have other detrimental effects on muscle tissue. For example, elevated $[Ca^{2+}]_i$ can impair autophagy (Pal et al., 2014), promote apoptosis (Hemmati-Brivanlou et al., 1994), induce malignant hyperthermia in susceptible individuals (Lopez et. al., 2018; Missiaen et. al., 2000), and contribute to muscle weakness and dysfunction (Anderssen et al., 2012; Chin et al., 2014;

Goswami et al., 2015; Jaiswal 2014; Pal et al., 2014). Perturbations in intracellular Ca^{2+} homeostasis are associated with numerous muscle pathologies, including juvenile myoclonic epilepsy, malignant hyperthermia, central core disease, and the muscle atrophy that occurs with diseases such as muscular dystrophy (MD; Anderssen et al., 2012, Mukherjee and Brooks 2014), amyotrophic lateral sclerosis (ALS; Chin et al., 2014; Goswami et al., 2015; Jaiswal 2014), cancer cachexia, diabetes, and sepsis (Costelli et al., 2005; Missiaen et al., 2000) as well as the atrophy that occurs with normal aging (Averna et al., 2001; Blalock et al., 1999; Costelli et al., 2005; Romero et al., 2002). Ca^{2+} dysregulation may also contribute to muscle necrosis in some forms of muscular dystrophy (Burr and Molkentin 2015). These negative consequences of aberrant $[Ca^{2+}]_i$ levels in skeletal muscle reflect the tight regulation of $[Ca^{2+}]_i$ in terms of time, space and amplitude required for normal muscle homeostasis and function (Costelli et. al., 2005; Lanner et al., 2010). Additionally, because ERG1a channels are also found in other tissues (e.g., brain, islet cells, tumor cells, heart, etc.) (Hardy et al., 2009; Pond et al., 2000; Perez-Neut et al., 2015), research of this mechanism may ultimately have a broader effect, addressing Ca^{2+} dysregulation in other tissues (Brawek and Garaschuk, 2014; Cheng et al., 2015; Sama and Norris 2013; Wang et al., 2014).

In summary, this study provides a potential mechanism to explain how upregulation of ERG1A might drive atrophy in skeletal muscle via downregulation of CaSeq1 protein levels, and subsequent amplification of SOCE, ECCE, and enhanced Ca^{2+} release from the SR via RyR1. Even though ERG1A is not a tractable pharmacological target for treatment of atrophy, a greater understanding of this mechanism could identify more suitable targets for development of therapies for numerous skeletal muscle pathologies.

ACKNOWLEDGEMENTS

The research reported in this publication was supported in large part by the Department of Defense office of the Congressionally Directed Medical Research Programs through a Peer Reviewed Medical Research Program (PRMRP) Discovery Award to ALP and GHH. The Southern Illinois University Carbondale (SIUC) Graduate School provided some financial support through funding to graduate students CW and SG. SIUC also provided some support through an Undergraduate Research-Enriched Academic Challenge (REACH) Award to OK. The Southern Illinois School of Medicine provided some financial support through their Medicine Mentor Professional Enrichment Experience Program to NM.

REFERENCES

1. Anderson LB, Hameed S, Latour CD, Latour SM, Graham VM, Hashmi MN, Cobb B, Dethrow N, Urazaev AK, Ravara B, Davie JK, Albertin G, Carraro U, Zampieri S, Pond AL. MERG1A Protein Abundance Increases in the Atrophied Skeletal Muscle of Denervated Mice, but does not Affect NFκB Activity. 2021. *Journal of Neuropathology and Experimental Neurology*. 80(8):776-788. doi: 10.1093/jnen/nlab062.

2. Andersson DC, Meli, AC, Reiken S, Betzenhauser MJ, Umanskaya A, Shiomi T, D'Armiento J, Marks AR. Leaky ryanodine receptors in β-sarcoglycan deficient mice: a potential common defect in muscular dystrophy. Skeletal Muscle 2:9-15, 2012.

3. Averna M, de Tullio R, Salamino F, Minafra R, Pontremoli S, Melloni E. Age-dependent degradation of calpastatin in kidney of hypertensive rats. J Biol Chem 276:38426-38432, 2001.

4. Bal NC, Maurya SK, Sopariwala DH, Sahoo SK, Gupta SC, Shaikh SA, Pant M, Rowland LA, bombardier E, Goonasekera SA, Tupling AR, Molkentin JD, Periasamy M. Nat Med 18:1575-1579, 2012.

5. Beard NA, Casarotto MG, Wei L, Varsanyi M, Laver DR, Dulhunty AF. Regulation of ryanodine receptors by calsequestrin: effect of high luminal Ca^{2+} and phosphorylation, Biophys. J. 88 (2005) 3444–3454.

6. Beard NA, Sakowska MM, Dulhunty AF, Laver DR. Calsequestrin is an inhibitor of skeletal muscle ryanodine receptor calcium release channels, Biophys. J. 82 (2002) 310–320.

7. Blalock EM, Porter NM, Landfield PW. Decreased G-protein-mediated regulation and shift in calcium channel types with age in hippocampal cultures. J Neurosciences 19:8674-684, 1999.

8. Boncompagni S, Protasi F, Franzini-Armstrong C. Sequential stages in the age dependent gradual formation and accumulation of tubular aggregates in fast twitch muscle fibers: SERCA and calsequestrin involvement. Age (Dordr) 2012;34(1):27-41. doi: 10.1007/s11357-001-9211-y.

9. Boncompagni S, Michelucci A, Pietrangelo L, Dirksen RT, Protasi F. Addendum: Exercise-dependent formation of new junctions that promote STIM1-Orai1 assembly in skeletal muscle. Sci Rep 2018;8(1):17463. Doi: 10.1038/s41598-018-33063-0.

10. Brawek B, Garaschuk O. Network-wide dysregulation of calcium homeostasis in Alzheimer's disease. Cell Tissue Res 357:427-438, 2014.

11. Bruton JD, aydin J, Yamada T, Shabalina IG, Ivarsson N, Zhang SJJ, Wada M, tavi P, Nedergaard J, Katz A, Westerblad H. Increased fatigue resistance linked to Ca2+-stimulated mitochondrial biogenesis in muscle fibers of cold-acclimated mice. J Physiol (Lond) 588:4275-4288, 2010.

12. Burr AR, Molkentin JD. Genetic evidence in the mouse solidifies the calcium hypothesis of myofibers death in muscular dystrophy. Cell Death and Differentiation doi:10.1038/cdd.2015.65, 2015.

13. Cheng AJ, Andersson DC, Lanner JT. Can't live with or without it: calcium and its role in Duchenne muscular dystrophy-induced muscle weakness. Am J Physiol Cell Physiol. 308:C697-C698, 2015.

14. Cherednichenko G, Hurne A, Lee EH, Fessenden JD, Allen PD, Beam KG, Pessah IN. Conformational activation of calcium entry by depolarization of skeletal myotubes. PNAS 2004;101:15793-15798.

15. Cherednichenko G, Ward CW, Feng W, Cabrales E, Michaelson L, Samso M, Lopez JR, Allen PD, Pessah IN. Enhanced excitation-coupled calcium entry in myotubes expressing malignant hyperthermia mutation R163C is attenuated by dantrolene. Molec. Pharmacol. 2008;73:1203-1212. doi: 10.1124/mol.107.043299.

16. Chin ER, Chen D, Bobyk KD, Mazala DAG. Perturbations in intracellular calcium handling in skeletal muscle in the G93A*SOD1 mouse model of amyotrophic lateral sclerosis. Am J Physiol Cell Physiol 307:C1031-1038, 2014.

17. Cho CH, Woo JS, Perez CF, Lee EH. A focus on extracellular Ca^{2+} entry into skeletal muscle. Exp. Molec. Medicine. 2017;49:e378. Doi: 10.1038/emm.2017.208.

18. Costelli P, Reffo P, Penna F, Autelli R, Bonelli G, Baccino FM. Ca^{2+}-dependent proteolysis in muscle wasting. Int J Biochem Cell Biol 37:2134-2146, 2005.

19. Curran ME, Splawski I, Timothy KW, Vincent GM, Green ED, Keating MT. A molecular basis for cardiac arrhythmia: herg mutations cause long QT syndrome. Cell 80:795-803, 1995.

20. Dainese M, Quarta M, Lyfenko AD, Paolini C, Canato M, Reggiani C, Dirksen RT, Protasi F. Anesthetic- and heat-induced sudden death in calsequestrin-1-knockout mice. FASEB 2009;23:1710-1720. Doi: 10.1096/fj.08-121335.

21. Dirksen RT. Checking your SOCCs and feet: the molecular mechanisms of Ca^{2+} entry in skeletal muscle. J Physiol. 2009;13:3139-3147.

22. Feske S, Gwack Y, Prakriya M, Srikanth S, Puppel SH, Tanasa B, Hogan PG, Lewis RS, Daly M, Rao A. A mutation in Orai1 causes immune deficiency by abrogating CRAC channel function. Nature 2006;441:179-185.

23. Fischer MJ, Paulussen JJ, Tollenaere JP, De Mol NJ, Janssen LH. Structure-activity relationships of astemizole derivatives for inhibition of store operated Ca2+ channels and exocytosis. Euro J Pharmacol 1998;350(2-3):353-361. doi: 10.1016/s0014-2999(98)00270-2.

24. Gach MP, Cherednichenko G, Haarman C, Lopez JR, Beam KG, Pessah IN, Franzini-Armstrong C, Allen PD. Alpha2delta1 dihydropyridine receptor subunit is a critical element for excitation-coupled calcium entry but not for formation of tetrads in skeletal myotubes. Biophys J 2008;94:3023-3034.

25. Goswami A, Jesse CM, Chandrasekar A, Bushuven E, Vollrath JT, Dreser A, Katona I, Beyer C, Johann S, Feller AC, Grond M, Wagner S, Nikolin S, Troost D, Weis J. Accumulation of STIM1 is associated with the degenerative muscle fibre phenotype in ALS and other neurogenic atrophies. Neuropath Appl Neurobiol 41:304-318, 2015.

26. Hardy AB, Manning Fox JE, Giglou PR, Wijesekara N, Bhattacharjee A, Sultan S, Gyulkhandanyan AV, Gaisano HY, MacDonald PE, Wheeler MB. Characterization of Erg K^+ channels in α- and β-cells of mouse and human islets. J Biol Chem 284(44): 30441–30452, 2009.

27. Hemmati-Brivanlou A, Kelly OG, Melton DA. Follistatin, an antagonist of activin, is expressed in the Spemann organizer and displays direct neuralizing activity. Cell 77:283-95, 1994.

28. Herzog A, C. Szegedi, I. Jona, F.W. Herberg, M. Varsanyi, Surface plasmon resonance studies prove the interaction of skeletal muscle sarcoplasmic reticular Ca^{2+} release channel/ryanodine receptor with calsequestrin, FEBS Lett. 472 (2000) 73–77.

29. Hockerman GH, Swarringin NM, Hameed S, Doran M, Jaeger C, Wang W-H, Pond AL. The Ubr2 gene is expressed in skeletal muscle atrophying as a result of hind limb suspension, but not Merg1a expression alone. Eur J Translational Myol 24(2):207-214, 2014. PMCID: PMC4163950.

30. Hurne AM, O'Brien JJ, Wingrove D, Cherednichenko G, Allen PD, Beam KG, Pessah IN. Ryanodine receptor type 1 (RYR1) mutations C4958S and C4961S reveal excitation-coupled calcium entry (ECCE) is independent of sarcoplasmic reticulum store depletion. J Biol Chem 2005;280:36994-37004.

31. Jaiswal MK. Selective vulnerability of motoneuron and perturbed mitochondrial calcium homeostasis in amyotrophic lateral sclerosis: Implications for motoneurons specific calcium dysregulation. Mol Cell Ther 2:26-32, 2014. Doi: 10.1186/2052-8426-2-26.

32. Jeong SY, Oh MR, Choi JH, Woo JS, Lee EH. Calsequestrin 1 is an active partner of stromal interaction molecule 2 in skeletal muscle. Cells 2021;10:2821. doi.org/10.3390/cells10112821.

33. Jones EMC, Roti Roti EC, Wang J, Delfosse SA, Robertson GA. Cardiac IKr channels minimally comprise hERG1a and 1b subunits. J Biol Chem 279:44690-44694, 2004.

34. Jones DK, Liu F, Vaidyanathan R, Eckhardt LL, Trudeau MC, Robertson GA. hERG 1b is critical for human cardiac repolarization. PNAS 2014;111:18073-77. Doi:1073/pnas.1414945111.

35. Kurebayashi N, Ogawa Y. Depletion of Ca2+ in the sarcoplasmic reticulum stimulates Ca2+ entry into mouse skeletal muscle fibres. J Physiol 2001;533:185-199.

36. Lanner JT, Georgiou DK, Joshi AD, Hamilton SL. Ryanodine receptors: Structure, expression, molecular details, and function in calcium release. Cold Spring Harb Perspect Biol 2:a003996, 2010. Doi: 10.1101/cshperspect.a003996.

37. Lee EH, Cherednichenko G,Pessah IN, Allen PD. Functional coupling between TRPC3 and RyR1 regulates the expressions of key triadic proteins. J Biol Chem 2006;281:10042-10048.

38. Lees-Miller JP, Kondo C, Wang L, Duff HJ. Electrophysiological characterization of an alternatively processed ERG K^+ channel in mouse and human hearts. *Circulation Research* 81(5):719-726, 1997.

39. Lin EC, Holzem KM, Anson BD, Moungey BM, Balijepalli SY, Tester DJ, Ackerman MJ, Delisle BP, Balijepalli RC, January CT. Properties of WT and mutant hERG K(+)

channels expressed in neonatal mouse cardiomyocytes. Am J Physiol Heart Circ Physiol 298(6):H1842-1849, 2010.

40. London B, Trudeau MC, Newton KP, Beyer AK, Copeland NG, Gilbert DJ, Jenkins NA, Satler CA, Robertson GA. Two isoforms of the mouse *Ether-a-go-go*-related gene coassemble to form channels with properties similar to the rapidly activating component of the cardiac delayed rectifier K^+ current. *Circulation Research* 81:870-878, 1997.

41. Lopez JR, Kaura V, Diggle CP, Hopkins PM, Allen PD. Malignant hyperthermia, environmentl heat stress, and intracellular calcium dysregulation in a mouse model expressing the p.G2435R variant of RYR1. British J Anaesthesia. 2018;121(4):953-961. doi: 10.1016/j.bja.2018.07.008.

42. Lyfenko AD, Dirksen RT. Differential dependence of store-operated and excitation-coupled calcium entry in skeletal muscle on STIM1 and Orai1. J Physiol 2008;586:4815-4824.

43. Michelli A, Boncompagni S, Pietrangelo L, Takano T, Dirksen RT. Pre-assembled Ca^{2+} entry units and constitutively active Ca^{2+} entry in skeletal muscle of calsequestrin-1 knockout mice. J General Physiol 2020;152(10):e202012617. doi.org/10.1085/jgp.202012617.

44. Mosca B, Delbono O, Messi ML, Bergameli L, Wang Z-M, Vukcevic M, Lopez R, Treves S, Nishi M, Takeshima H, Paolini C, Martini M, Rispoli G, Protasi F, Zorzato F. Enhanced dihydropyridine receptor calcium channel activity restores muscle strength in JP45/CASQ1 double knockout mice. Nature Communications 2013;4:1541. doi: 10.1038/ncomms2496.

45. Mosca B, Eckhardt J, Bergamelli L, Treves S, Bongianino R, De Negri M, Priori SG, Protasi F, Zorzato F. Role of the JP45-calsequestrin complex on calcium entry in slow twitch skeletal muscles. J Biol Chem 2016;291(28):14555-14565.

46. Missiaen L, Robberecht W, van Den Bosch L, Callewaert G, Parys JB, Wuytack F, Raeymaekers L, Nilius B, Eggermont J, De Smedt H. Abnormal intracellular calcium homeostasis and disease. Cell Calcium 28:1-21, 2000.

47. Mukherjee S, Brooks WH. Stromal interaction molecules as important therapeutic targets in diseases with dysregulated calcium flux. Biochim Biophys Acta 1843:2307-2314, 2014. doi:10.1016/j.bbamer.2014.03.019.

48. Nelson BR, Wu F, Liu Y, Anderson DM, McAnally J, Lin W, Cannon SC, Bassel-Duby R, Olson EN. Skeletal muscle specific T-tubule protein STAC3 mediates voltage-induced Ca^{2+} release and contractility. PNAS 2013;110(29):11881-11886. Doi: 10.1073/pnas.1310571110/-/DCSupplemental.

49. Olivera JF, Pizarro G. Two inhibitors of store operated Ca^{2+} entry suppress excitation contraction coupling in frog skeletal muscle. J Muscle Res Cell Motil 2010;31:127-139.

50. Pal R, Palmieri M, Loehr J, Li S, Abo-Zahrah R, Monroe T, Thankur P, Sardiello M, Rodney G. Src-dependent impairment of autophagy by oxidative stress in a mouse model of Duschenne muscular dystrophy. Nat Commun 5:4425, 2014.

51. Paolini C, Quarta M, Nori A, Boncompagni S, Canato M, Volpe P, et al. Reorganized stores and impaired calcium handling in skeletal muscle of mice lacking calsequestrin-1. J Physiol. 2007;583(Pt 2):767–84. doi:10.1113/jphysiol.2007.138024.

52. Perez-Neut M, Shum A, Cuvas BD, Miller R, Gentile S. Stimulation of hERG1 channel activity promotes a calcium-dependent degradation of cyclin E2, but not cyclin E1, in breast cancer cells. Oncotarget 6:1631-1639, 2015.

53. Perni S, Close M, Franzini-Armstrong C. Novel details of calsequestrin gel conformation in situ. J Biol Chem 2013;288:31358-31362.

54. Pitake S, Ochs RS. Membrane depolarization increases ryanodine sensitivity to Ca^{2+} release to the cytosol in L6 skeletal muscle cells: Implications for excitation–contraction coupling. Exp. Biol. Med. 2015; 241(8):854-862. doi.org/10.1177/1535370215619

55. Pond AL, Nedele C, Wang W-H, Wang X, Walther C, Jaeger C, Bradley KS, Du H, Fujita N, Hockerman GH, Hannon KM. The MERG1a channel modulates skeletal muscle *MuRF1*, but not *MAFbx*, expression. *Muscle & Nerve.* 49(3):378-388, 2013. PMCID: PMC4056345.

56. Pond AL, Petrecca K, Van Wagoner DR, Shrier A, Nerbonne JM. Expression of distinct ERG proteins in rat, mouse and human heart: Relation to functional I_{Kr} channels. J Biol Chem 275:5997-6006, 2000. PMID: 10681594.

57. Protasi F, Girolami B, Serano M, Pietrangelo L, Paolini C. Ablation of calsequestrin-1 Ca^{2+} unbalance and susceptibility to heat stroke. Front Physiol 2022;13:1033300. doi:10.3389/fphys.2022.1033300.

58. Rasmussen HB, Moller M, Knaus H-G, Jensen BS, Olesen S-P, Jorgensen NK. Subcellular localization of the delayed rectifier K^+ channels KCNQ1 and ERG1 in the rat heart. Am J Physiol Heart Circ Physiol 286:H13-139, 2004.

59. Romero PJ, Salas V, Hernandez C. Calcium pump phosphoenzyme from young and old human red blood cells. Cell Biol Int 26:945-949, 2002.

60. Roos J, DiGregio PJ, Yeromin AV, Ohlsen K, Lioudyno M, Zhang S, Safrina O, Kozak JA, Wagner SL, Cahalan MD, Velcelebi G, Stauderman KA. STIM1, an essential and conserved component of store-operated Ca^{2+} channel function. J Cell Biol 2005;169:435-445.

61. Sama DM, Norris CM. Calcium dysregulation and neuroinflammation: Discrete and integrated mechanisms for age-related synaptic dysfunction. Ageing Res Rev 12:982-995, 2013.

62. Stiber J, Hawkins A, Zhang ZS, Wang S, Burch J, Graham V, Ward CC, Seth M, Finch E, Malouf N, Williams RS, Eu JP, Rosenberg P. STIM1 signaling controls store-operated calcium entry required for development and contractile function in skeletal muscle. Nat Cell Biol 2008;10:688-697.

63. Tu MK, Levin JB, Hamilton AM, Borodinsky LN. Calcium signaling in skeletal muscle development, maintenance and regeneration. Cell Calcium 2016;59:91-97.

64. Vig M, Peinelt C, Beck A, Koomoa DL, Rabah D, Koblan-Huberson M, Kraft S, Turner H, Fleig A, Penner R, Kinet JP. CRACM1 is a plasma membrane protein essential for store-operated calcium entry. Science 2006;312:1220-1223.

65. Wang X, Hockerman GH, Green 3rd HW, Babbs CF, Mohammad SI, Gerrard D, Latour MA, London B, Hannon KM, Pond AL. Merg1a K^+ channel induces skeletal muscle

atrophy by activating the ubiquitin proteasome pathway. FASEB J 20(9):1531-3, 2006. PMCID: 16723379.

66. Wang Y, Jarrard RE, Pratt EPS, Guerra ML, Salyer AE, Lange AM, Soderling IM, Hockerman GH. Uncoupling of Cav1.2 from Ca^{2+}-induced Ca^{2+} release and SK channel regulation in pancreatic β-cells. Mol Endocrinol 28:458-476, 2014.

67. Wang Q, Michalak M. Calsequestrin, structure, function, and evolution. Cell Calcium 2020;90:102242. doi.org/10.1016/j.ceca.2020.102242.

68. Wang L, Zhang L, Li S, Zheng Y, Yan X, Chen M, Wang H, Putney JW, Luo D. Retrograde regulation of STIM1-Orai1 interaction and store-operated Ca^{2+} entry by calsequestrin. Sci. Rep. 2015;5:11349.

69. Wei L, Hanna AD, Beard NA, Dulhunty AF. Unique isoform-specific properties of calsequestrin in the heart and skeletal muscle. Cell Calcium 2009;45:474-484. doi: 10.1016/j.cerca.2009.03.006.

70. Whitmore C, Pratt E, Anderson LB, Bradley K, Latour SM, Hashmi MN, Urazaev AK, Weilbacher R, Davie JK, Wang W-H, Hockerman GH, **Pond AL**. The ERG1a potassium channel increases basal intracellular calcium concentration and calpain activity in skeletal muscle cells. 2020. *Skeletal Muscle*. 10:1-15. doi.org/10.1186/s13395-019-0220-3.

71. Woo JS, Jeong SY, Park JH, Choi JH, Lee EH. Calsequestrin: A well-known but curious protein in skeletal muscle. Exp Molec Medicine 2020;52:1908-1925. doi.org/10.1038/s12276-020-00535-1.

72. Yang T, Allen PD, Pessah IN, Lopez JR. Enhanced excitation-coupled calcium entry in myotubes is associated with expression of RyR1 malignant hyperthermia mutations. J Biol Chem 2007;282:3747-37478.

73. Zampieri S, Sandri M, Cheatwood JL, Balaraman RP, Anderson LB, Cobb BA, Latour CD, Hockerman GH, Kern H, Sartori R, Ravara B, Merigliano S, da Dalt G, Davie JK, Kohli P, Pond AL. The ERG1A K^+ channel is more abundant in *Rectus abdominis* muscle from cancer patients than in that from healthy humans. 2021. *Diagnostics.* 11(10):1879. doi.org/10.3390/diagnostics11101879.

74. Zhang L, Wang L, Li S, Xue J, Luo D. Calsequestrin-1 regulates store-operated Ca^{2+} entry by inhibiting STIM1 aggregation. Cell Physiol Biochem. 2016;38:2183-2193. doi: 10.1159/000445574.

Figure 1. HERG does not enhance intracellular calcium concentration ($[Ca^{2+}]_i$) through modulation of the L-type channel in skeletal muscle. A. The increase in intracellular Ca^{2+} ($[Ca^{2+}]_i$) initiated by depolarization is significantly greater in myotubes expressing HERG relative to controls. B. Nifedipine (10 μM) has a significant inhibitory effect on the increase in $[Ca^{2+}]_i$ that occurs in control cells in response to depolarization over 90 seconds after addition of KCl. C. Nifedipine also inhibits a portion of the HERG-induced increase in $[Ca^{2+}]_i$ for up to 40 seconds. D. Nifedipine-sensitive currents do not differ significantly between the control and HERG-expressing myotubes, demonstrating that the HERG-modulated increase in $[Ca^{2+}]_i$ does not result from activation of L-type Ca^{2+} channels. $[Ca^{2+}]_i$ was evaluated by the ratiometric fluorescent Fura-2 dye and the 340/380 ratios were determined and normalized to baseline. The area under the curve was determined for indicated timepoints and analyzed by a 2 x 2 ANOVA design for repeated measures and the interaction between HERG and treatment was examined for statistical significance. The bars (A-C) and symbols (D) represent means and error bars represent standard error of the mean. n=16 (8 control and 8 HERG-expressing myotubes). *$p<0.05$, **$p<0.01$.

Figure 2. Gene expression, protein abundance, and current density of the Cav1.1 L-type Ca^{2+} channel are not affected by HERG expression in C_2C_{12} myotubes. A. Electrophysiology studies reveal that L-type Ca^{2+} channel current density is not affected by HERG expression. B,C. RT-qPCR assays reveal that mRNA levels of adult (B) and embryonic (C) Cav1.1 are not affected by HERG expression up to 60 hours post transduction with HERG encoded adenovirus. D,E. Immunoblot (D) and optical density measures (E) show that Cav1.1 protein abundance is not significantly affected at 48 hours post HERG expression. Data displayed in panels A and E were analyzed by Student's t-test while a one-way ANOVA was used to analyze the data in panels B and C. Bars represent mean and error bars represent standard error of the mean. (A. n=10; n=5 control and n=5 HERG-expressing myotubes; B,C. n=8, 4 control and 4 HERG-expressing samples; D,E. n=6, 3 control and 3 HERG-expressing myotube lysate samples.)

Figure 3. Excitation coupled calcium entry (ECCE) is a source of the greater increase in intracellular calcium concentration ($[Ca^{2+}]_i$) that occurs in response to depolarization by KCl in HERG-expressing cells. A. In control cells, 2-APB has an inhibitory effect on the initial mean increase in $[Ca^{2+}]_i$ that occurs in response to depolarization; the effect reverses over time. B. The 2-APB has a significant inhibitory effect on the HERG-modulated increase in $[Ca^{2+}]_i$ that occurs in response to depolarization. C. The initial 2-APB-sensitive currents differ significantly between the depolarized control and HERG-expressing myotubes, suggesting that a source of the initial HERG-modulated increase in $[Ca^{2+}]_i$ is extracellular. The $[Ca^{2+}]_i$ was evaluated by the ratiometric fluorescent Fura-2 dye and the 340/380 ratios were determined and normalized to baseline. The area under the curve was determined for indicated timepoints and analyzed by a 2 x 2 ANOVA design for repeated measures and the interaction between HERG and treatment was examined for statistical significance. The bars (A,B) and symbols (C) represent means and error bars represent standard deviation. n=24 (12 control and 12 HERG-expressing myotubes). *$p<0.05$, **$p<0.01$.

Figure 4. HERG modulates SOCE. A. HERG expressing myotubes exhibit a significantly greater increase in intracellular Ca^{2+} concentration ($[Ca^{2+}]_i$) than control cells when treated with high Ca^{2+} (2.5 mM $CaCl_2$) after depletion of SR Ca^{2+} stores by thapsigargin (1 μM); this response is significantly inhibited by the SOCE inhibitor 2-APB (100 μM). B. Representative line graph of a single assay. The $[Ca^{2+}]_i$ was evaluated by ratiometric fluorescent Fura-2 dye and the 340/380 ratios were determined and normalized to baseline. AUCs were calculated per treatment group and analyzed by one-way ANOVA. Means were separated by Tukey's test. The bars (A) and symbols (B) represent means and error bars represent standard error of the mean. n=4 dates of 24 wells each (12 wells of HERG-expressing myotubes and 12 wells of controls).

Figure 5. Sarcoplasmic reticulum Ca^{2+} stores is a source of the greater increase in intracellular Ca^{2+} concentration ($[Ca^{2+}]_i$) that occurs in response to depolarization by KCl (100 mM) in HERG-expressing cells. A. In control cells, thapsigargin has no significant effect on $[Ca^{2+}]_i$ in response to depolarization. B. Thapsigargin (1 μM) has a significant inhibitory effect on the HERG-modulated increase in $[Ca^{2+}]_i$ that occurs in response to depolarization. C. Thapsigargin-sensitive currents differ significantly between the depolarized control and HERG-expressing myotubes, suggesting that HERG may also affect release of Ca^{2+} from intracellular stores. The $[Ca^{2+}]_i$ was evaluated by the ratiometric fluorescent Fura-2 dye and the 340/380 ratios were determined and normalized to baseline. The areas under the curve (AUCs) were determined for indicated timepoints and analyzed by a 2 x 2 ANOVA design for repeated measures and the interaction between HERG and treatment was examined for statistical significance. The bars (A,B) represent mean AUCs and symbols (C) represent mean $[Ca^{2+}]_i$ and error bars represent standard error of the mean. n=20 (10 control and 10 HERG-expressing myotubes). *$p<0.05$.

Figure 6. HERG modulates ryanodine receptor-mediated Ca^{2+} release. A. HERG expressing myotubes exhibit a significantly greater increase in intracellular concentration ($[Ca^{2+}]_i$) than control cells when treated with caffeine (5 mM); this response is significantly inhibited by ryanodine (90 uM to inhibit ryanodine receptors) in HERG-expressing, but not control myotubes. n=4 dates of 24 wells each (12 wells of HERG-expressing myotubes and 12 wells of controls). B. Representative line graph of a single assay of 24 wells. n=24; the 24 wells consisted of 3 wells per each of six groups. The $[Ca^{2+}]_i$ was evaluated by ratiometric fluorescent Fura-2 dye and the 340/380 ratios were determined and normalized to baseline. Areas under the curve (AUCs) were analyzed by one-way ANOVA and means were separated by Tukey's test. The bars (A) and symbols (B) represent means and error bars represent standard error of the mean (A) and standard deviation (B).

Figure 7. Calsequestrin1 (CaSeq1) mRNA and protein levels are reduced in C_2C_{12} myotubes 48 hours after treatment with HERG encoded virus relative to myotubes treated with control virus. A. Fold changes in HERG and CaSeq1 mRNA levels in response to transduction with HERG-encoded adenovirus. HERG mRNA increases 2.6-fold ($p<0.02$) in HERG-transduced myotubes and CaSeq1 mRNA decreases 0.83-fold ($p<0.05$) in the HERG-expressing cells. B. Control and HERG-expressing myotube lysates immunoblotted with antibody specific for CaSeq1 protein. C. Control and HERG-expressing myotube lysates immunoblotted with antibody specific for the "house-keeping" protein GAPDH. D. PVDF membrane stained with Coomassie blue to confirm equal sample loading in lanes. E. Normalized optical densities (OD) of individual CaSeq1 proteins and of CaSeq1 proteins combined ("Total") from immunoblot. Mean ODs of control and HERG-expressing cells (within each protein) were analyzed by Student's T-test. Bars represent average OD and error bars denote the standard deviation. n=8, 4 control groups and 4 HERG-expressing groups. Skm = mouse skeletal muscle.

Figure 8. HERG increases intracellular Ca^{2+} concentration by decreasing abundance of the Ca^{2+} binding/buffering protein CalSequestrin 1. Two important questions are: A) How does ERG1A decrease Calsequestrin 1?; and B) What induces increased levels of the ERG1A channel itself?

Table 1. Primer sequences for RT-qPCR.

	Primer Sequence 5' – 3'	**Size (bp)**	**Tm (°C)**	**GC (%)**	**Amplicon Size (bp)**
Merg1a Forward	cctcgacaccatcatccgca	20	59.6	55.0	145
Merg1a Reverse	aggaaatcgcaggtgcaggg	20	60.3	60.0	
Calsequestrin 1 Forward	atgagagctaccgacaggatg	21	56.3	55	105
Calsequestrin 1 Reverse	caccgtcgtactcagggaag	20	54.4	50	
GAPDH Forward	actcccactcttccaccttc	20	56.3	55	272
GAPDH Reverse	ctaggcccctcctgttattatg	22	54.4	50	

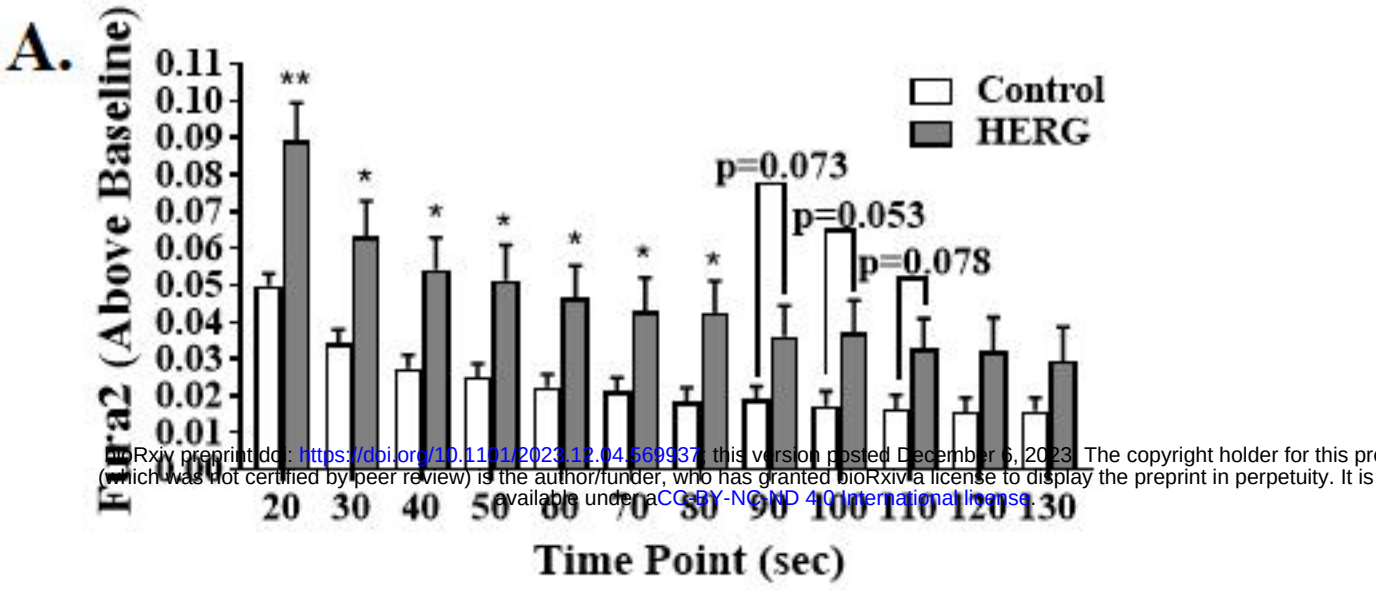

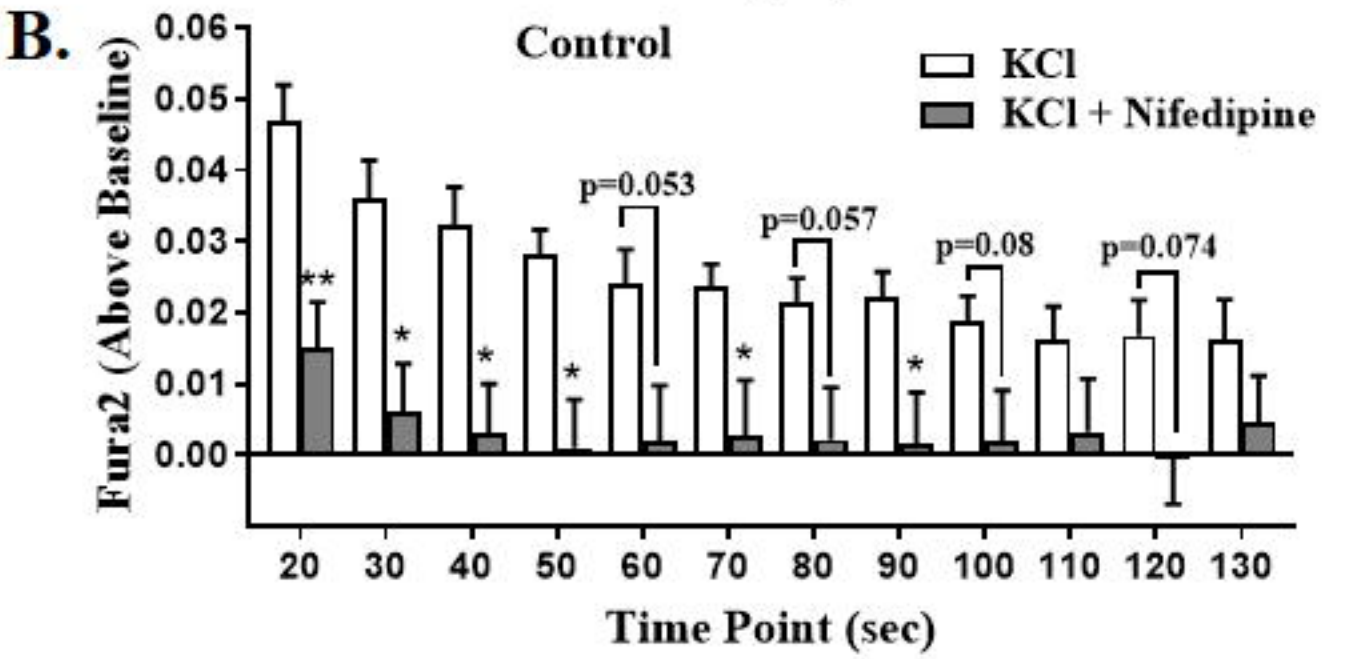

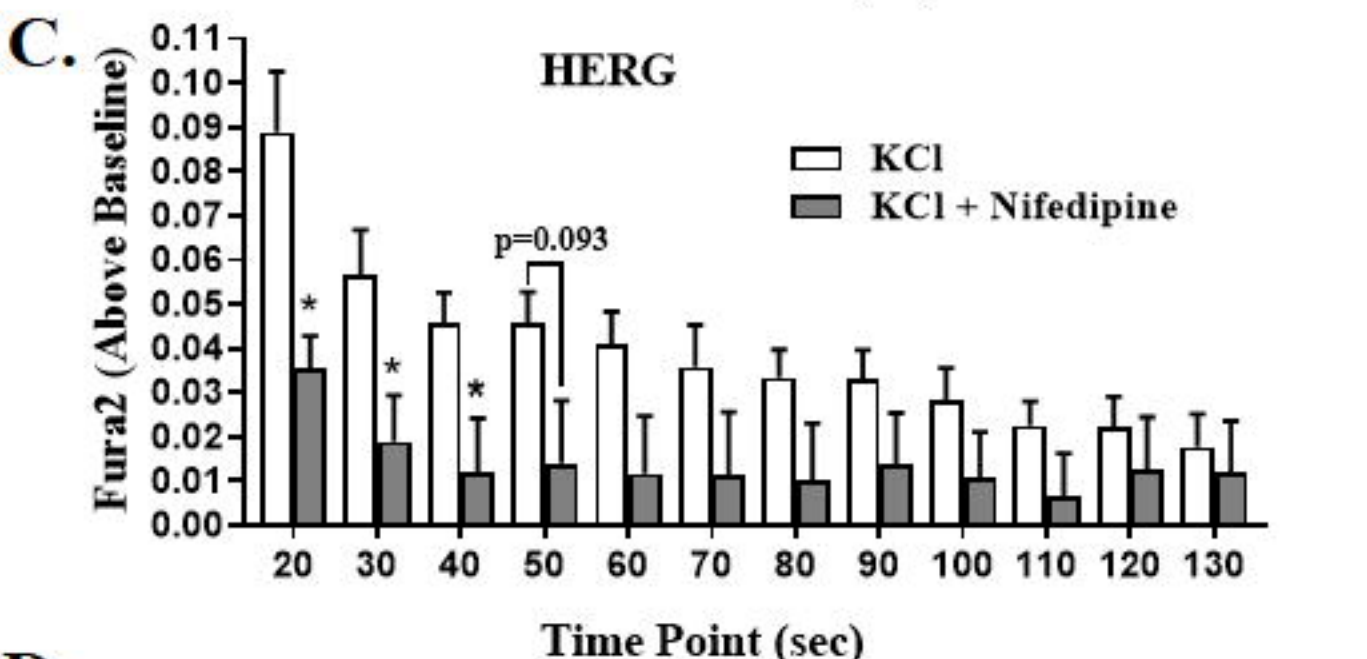

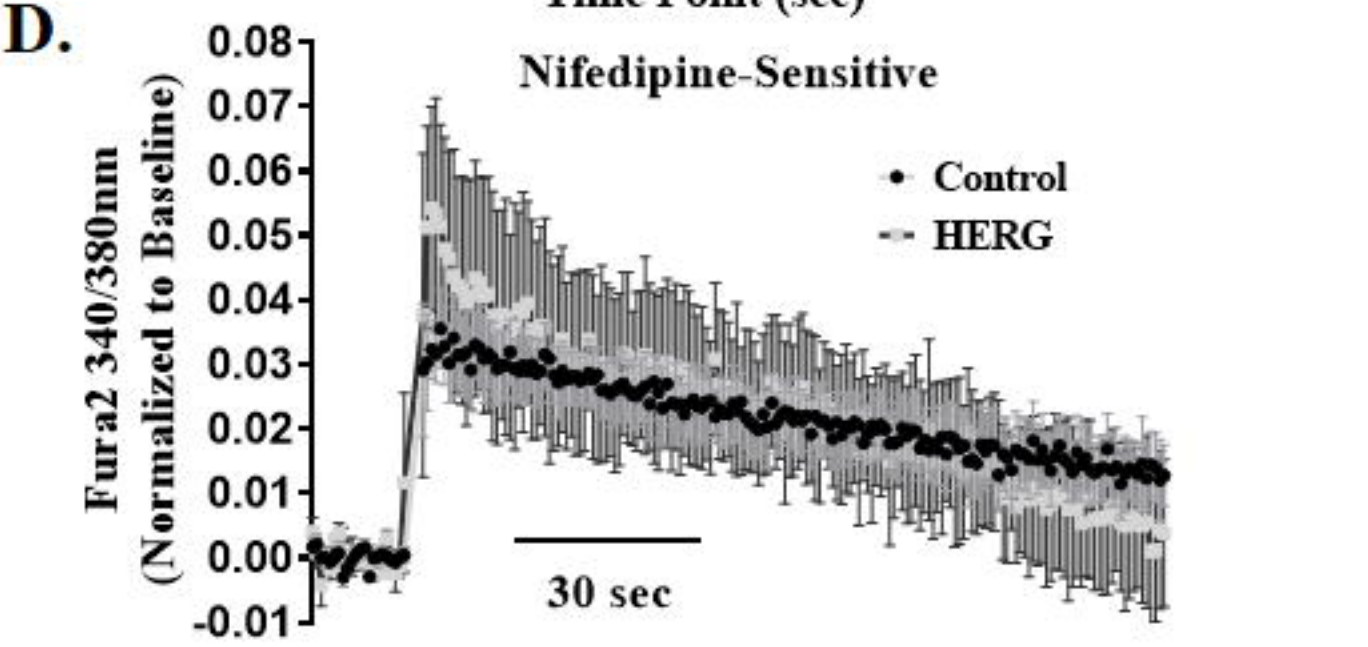

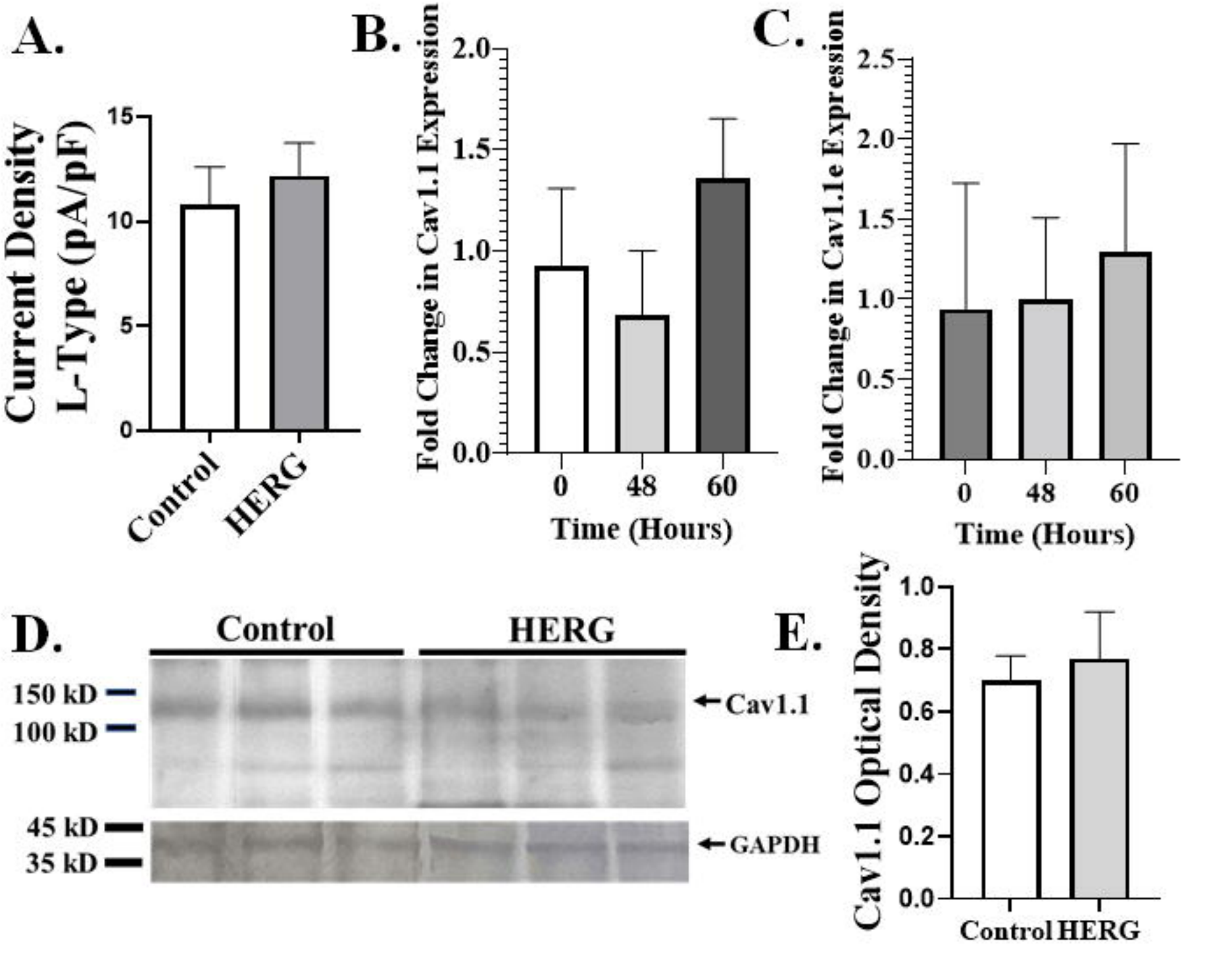
A.
Current Density
L-Type (pA/pF)
15
10
5
0
Control
HERG
B.
Fold Change in Cav1.1 Expression
2.0
1.5
1.0
0.5
0.0
0
48
60
Time (Hours)
C.
Fold Change in Cav1.1e Expression
2.5
2.0
1.5
1.0
0.5
0.0
0
48
60
Time (Hours)
D.
Control
HERG
150 kD
100 kD
45 kD
35 kD
Cav1.1
GAPDH
E.
Cav1.1 Optical Density
1.0
0.8
0.6
0.4
0.2
0.0
Control
HERG

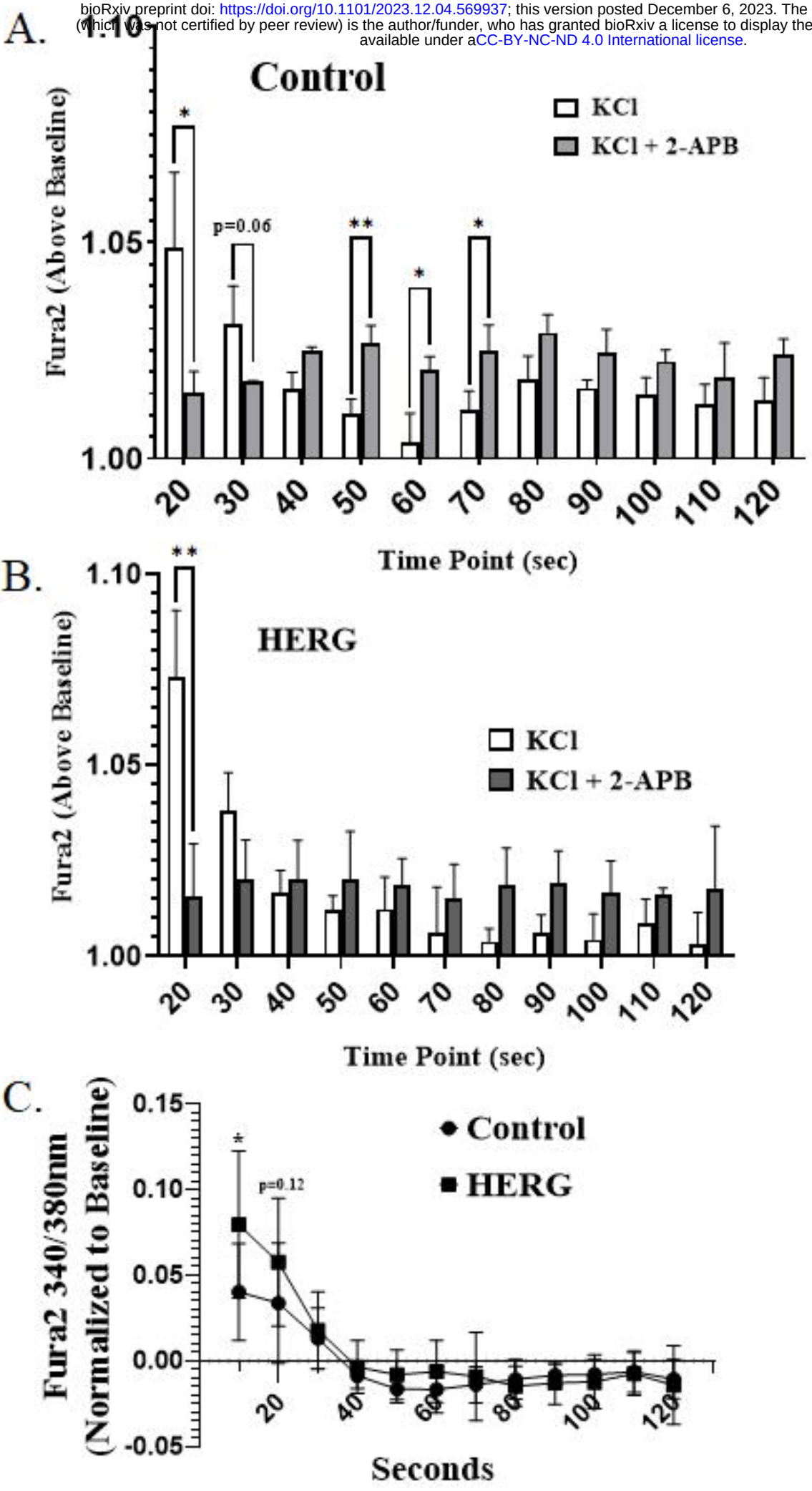

A.

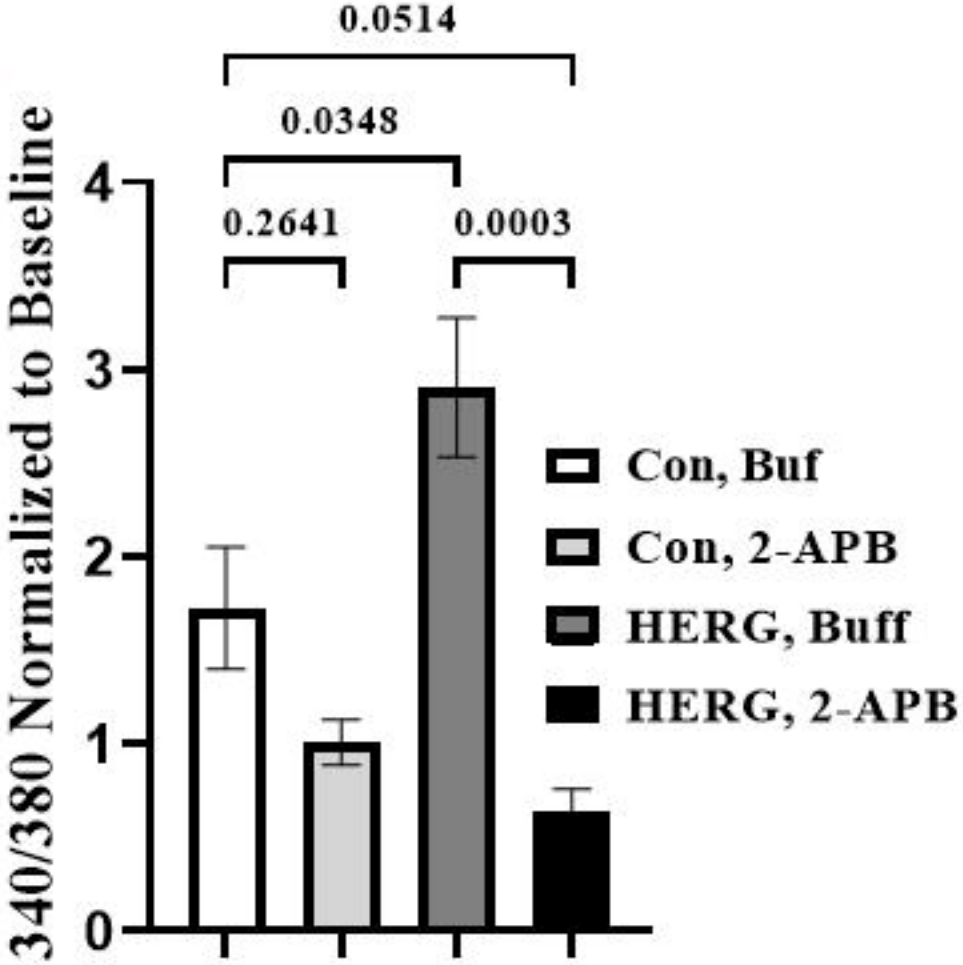
0.0514
0.0348
0.2641
0.0003
340/380 Normalized to Baseline
0
1
2
3
4
Con, Buf
Con, 2-APB
HERG, Buff
HERG, 2-APB

B.

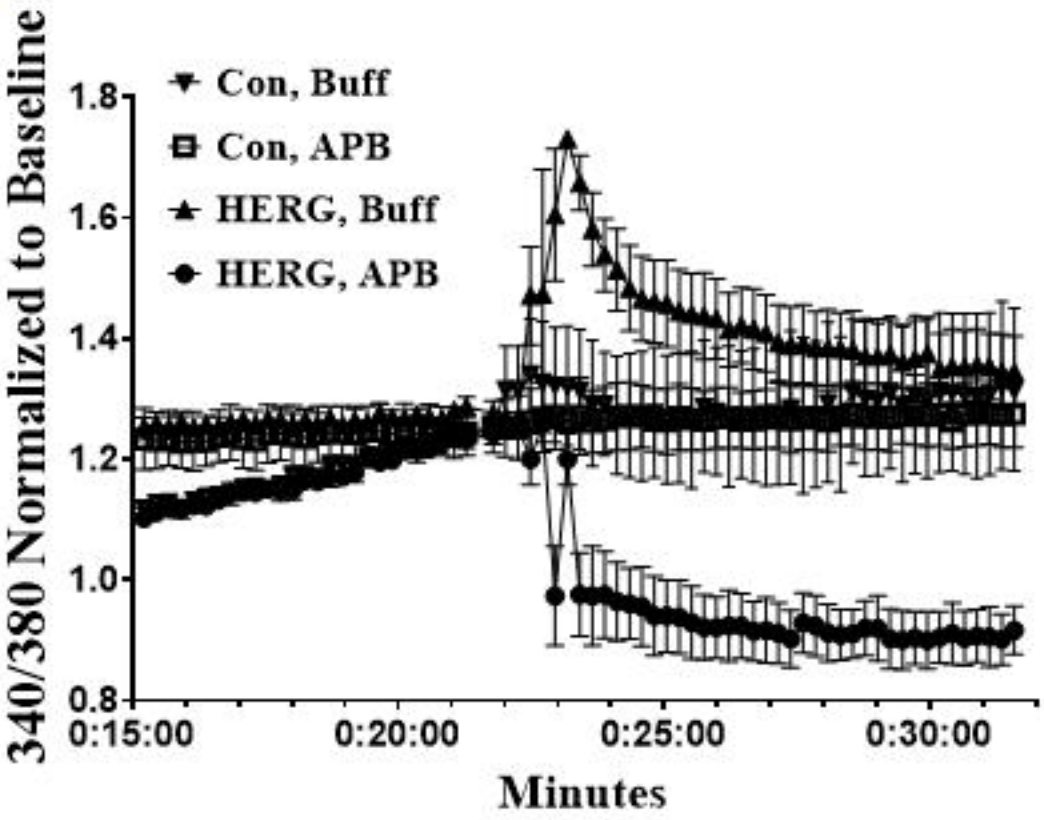
Con, Buff
Con, APB
HERG, Buff
HERG, APB
340/380 Normalized to Baseline
0.8
1.0
1.2
1.4
1.6
1.8
0:15:00
0:20:00
0:25:00
0:30:00
Minutes

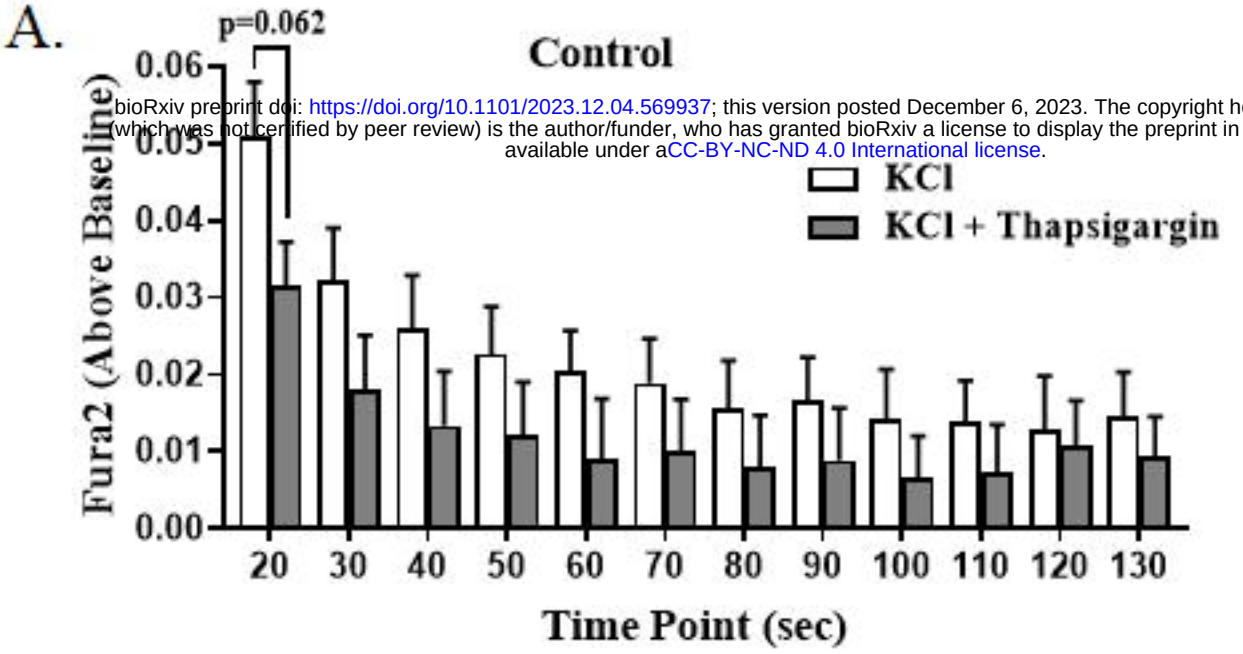

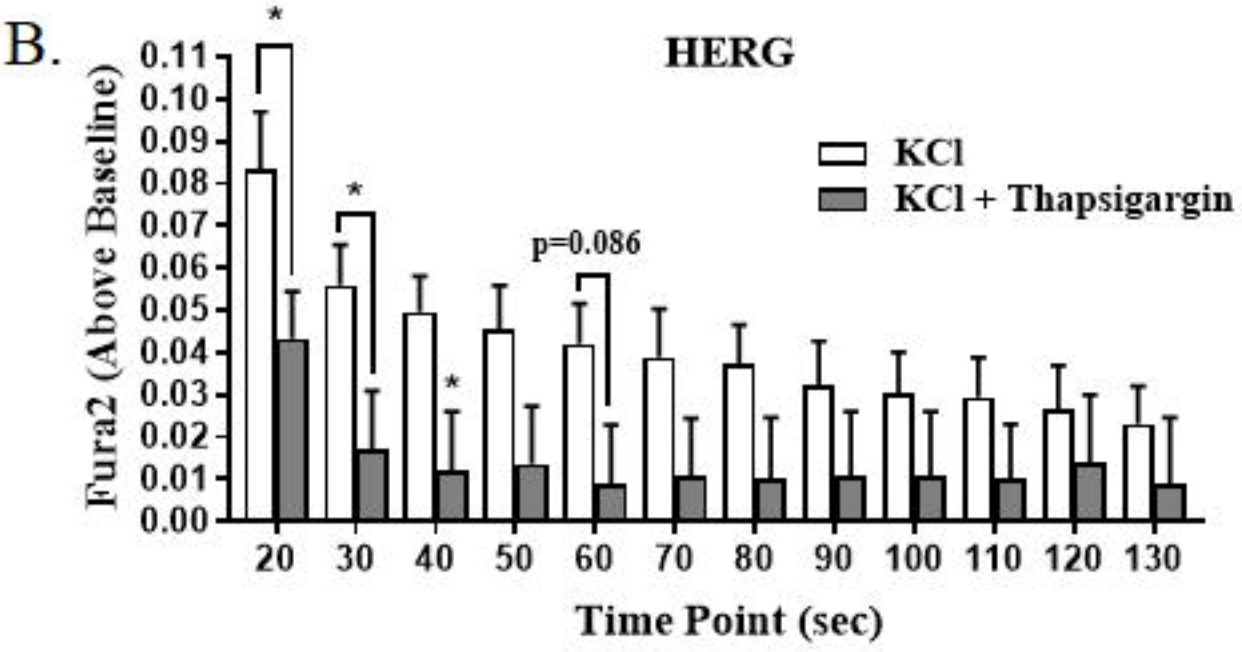

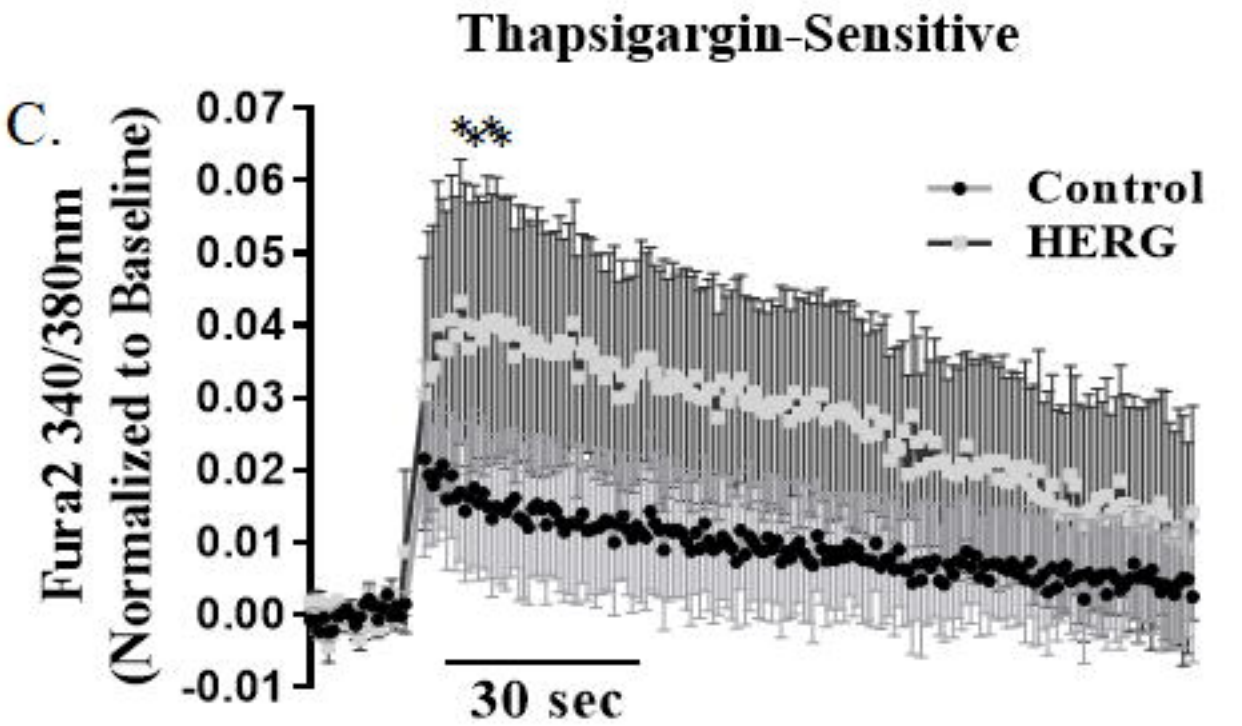

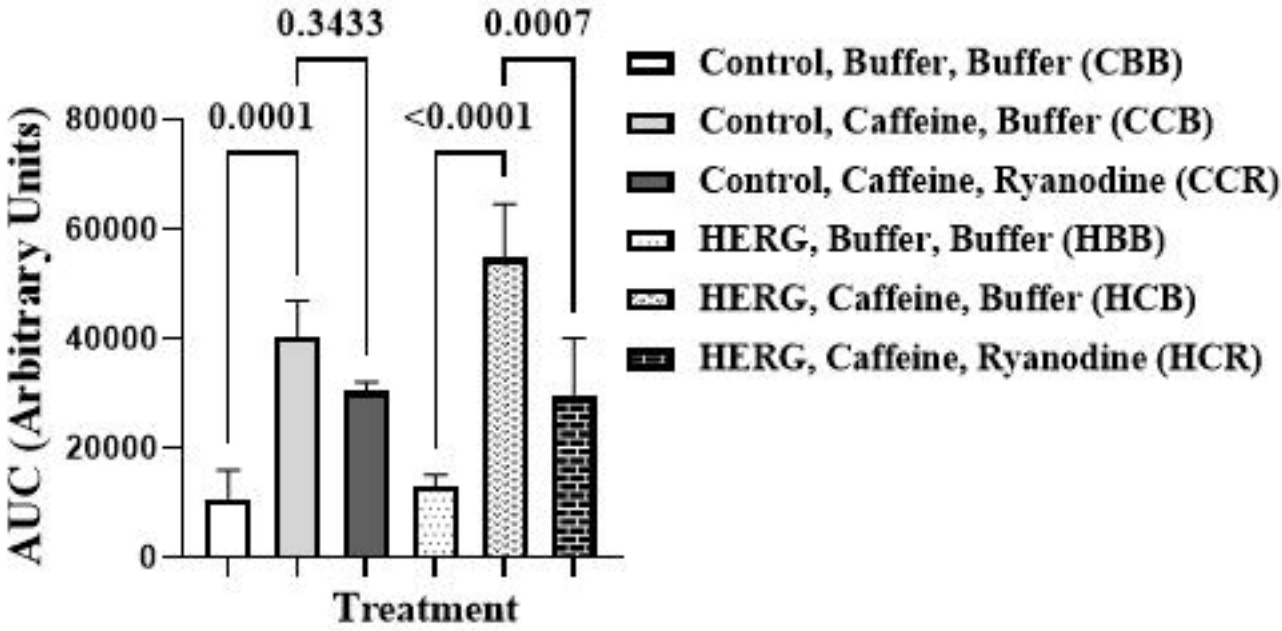
0.3433
0.0007
0.0001
<0.0001
80000
60000
40000
20000
0
AUC (Arbitrary Units)
Treatment
Control, Buffer, Buffer (CBB)
Control, Caffeine, Buffer (CCB)
Control, Caffeine, Ryanodine (CCR)
HERG, Buffer, Buffer (HBB)
HERG, Caffeine, Buffer (HCB)
HERG, Caffeine, Ryanodine (HCR)

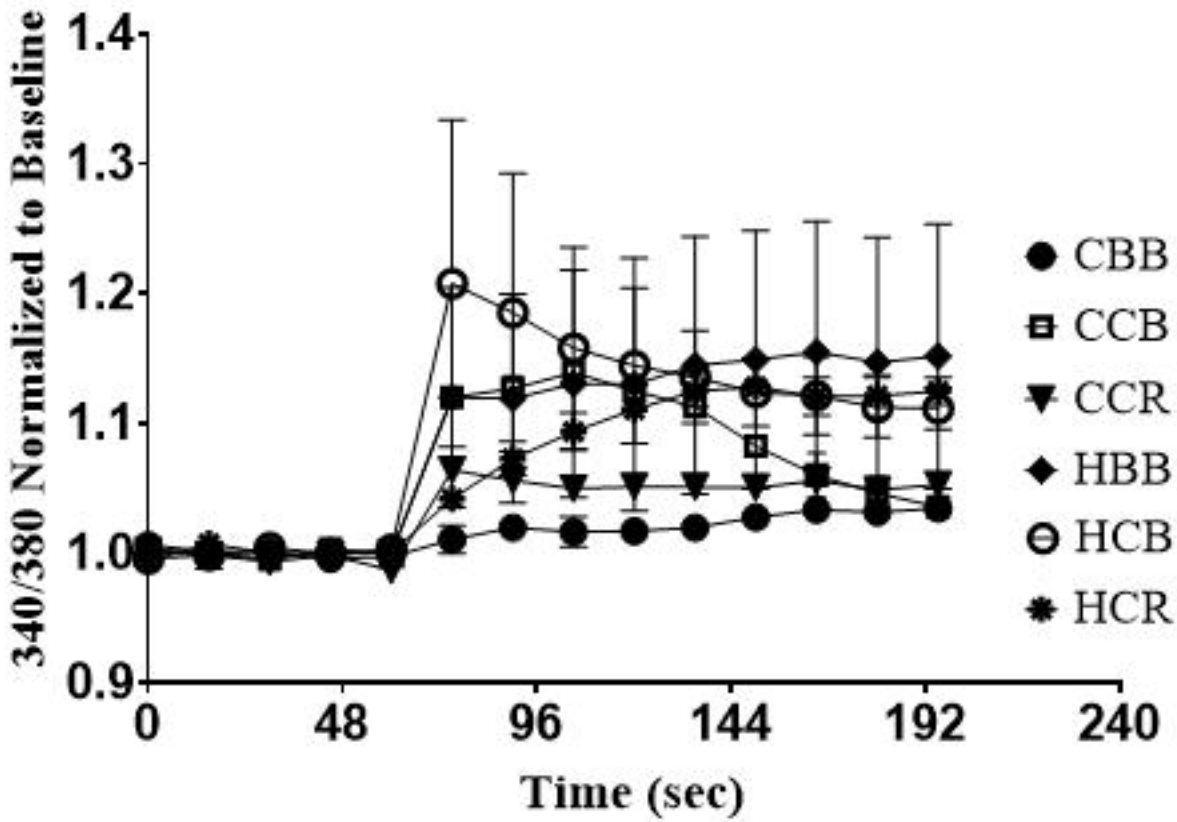
340/380 Normalized to Baseline
1.4
1.3
1.2
1.1
1.0
0.9
0
48
96
144
192
240
Time (sec)
CBB
CCB
CCR
HBB
HCB
HCR

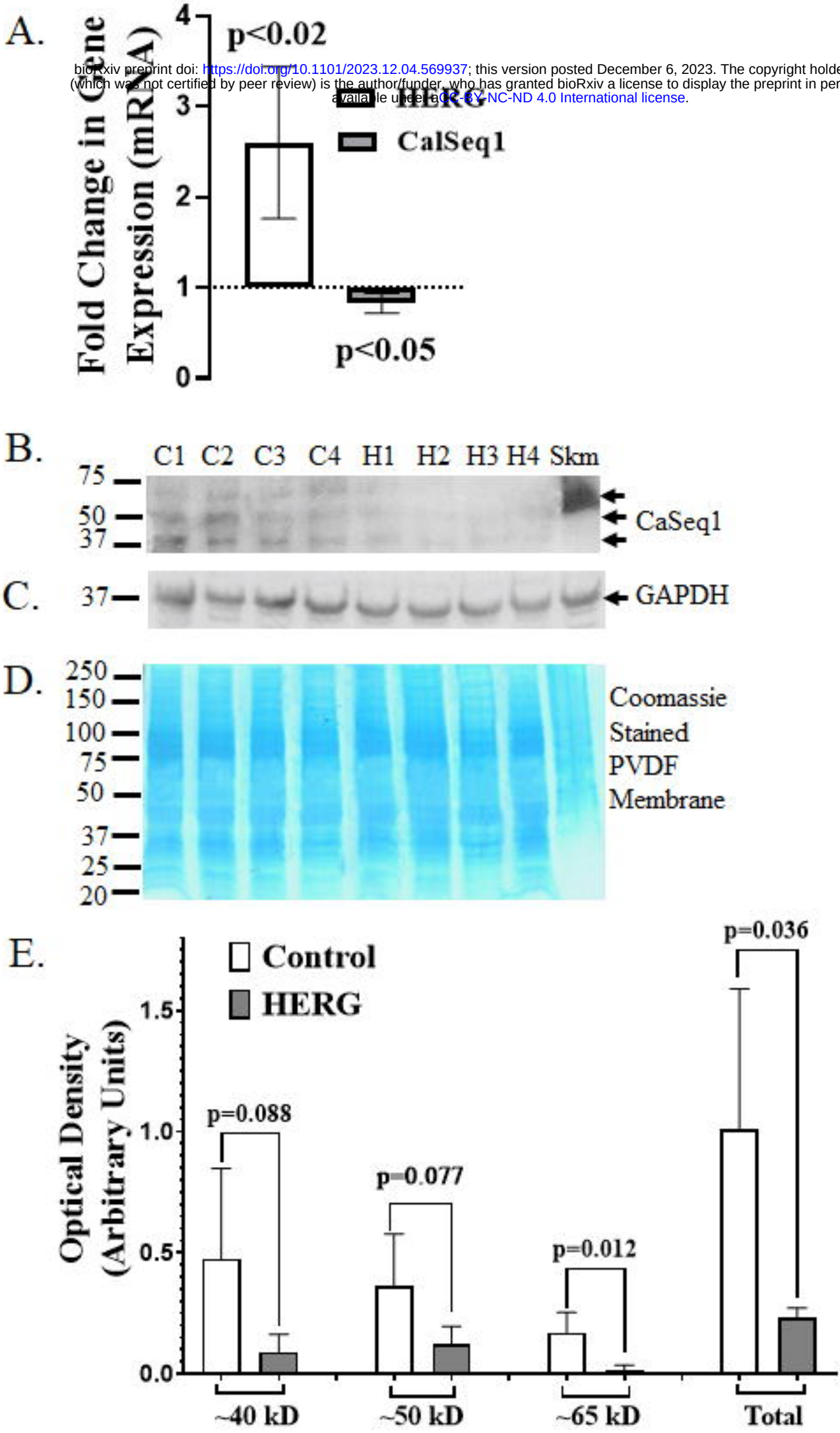

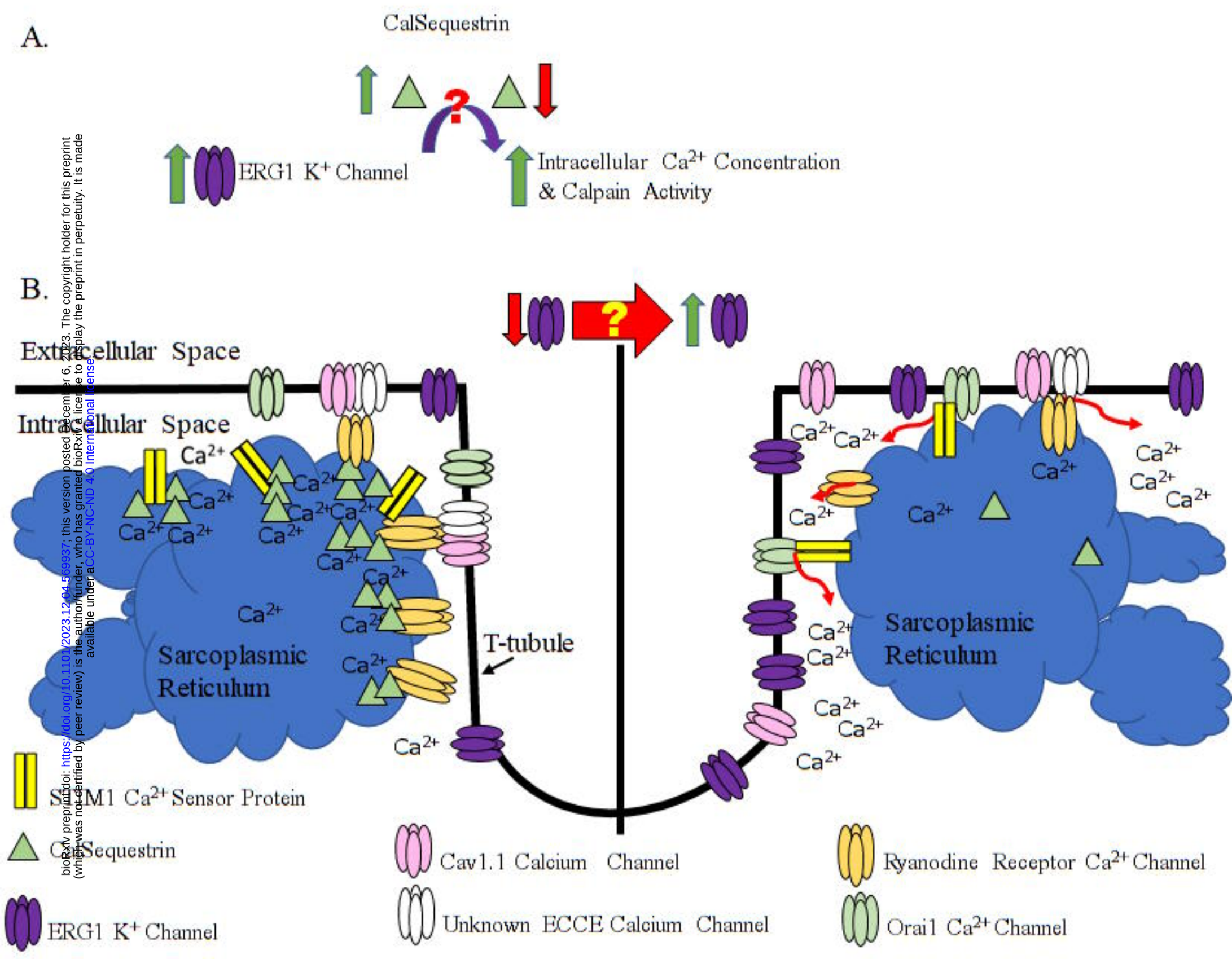

Table 1. Primer sequences for RT-qPCR.

	Primer Sequence 5' – 3'	**Size (bp)**	**Tm (°C)**	**GC (%)**	**Amplicon Size (bp)**
Merg1a Forward	cctcgacaccatcatccgca	20	59.6	55.0	145
Merg1a Reverse	aggaaatcgcaggtgcaggg	20	60.3	60.0	
Calsequestrin 1 Forward	atgagagctaccgacaggatg	21	56.3	55	105
Calsequestrin 1 Reverse	caccgtcgtactcagggaag	20	54.4	50	
GAPDH Forward	actcccactcttccaccttc	20	56.3	55	272
GAPDH Reverse	ctaggcccctcctgttattatg	22	54.4	50	